Naturally Occurring Polymorphisms in Human Cytomegalovirus gO Exert Epistatic Influences on Cell-Free and Cell-To-Cell Spread, and Antibody Neutralization on gH Epitopes.

Le Zhang Day[3,4], Cora Stegmann[1,4], Eric P. Schultz [1, 2, 4], Jean-Marc Lanchy[1,4], Qin Yu[1,4] , and Brent J. Ryckman[1,2,3,4]*

Division of Biological Sciences[1], Cellular, Molecular and Microbial Biology Program[2], Biochemistry and Biophysics Program[3], Center for Biomolecular Structure and Dynamics[4], University of Montana, Missoula, Montana, U.S.A.

*Corresponding author: Dr. Brent J. Ryckman
Division of Biological Sciences
Interdisciplinary Science Building Rm. 215
The University of Montana
Missoula, MT 59812
Tel: 406-243-6948
Fax: 406-243-4304
Email: brent.ryckman@mso.umt.edu

Running Title: Epistatic effects of HCMV gO polymorphisms

ABSTRACT

The human cytomegalovirus (HCMV) glycoproteins H and L (gH/gL) can be bound by either gO, or the UL128-131 proteins to form complexes that facilitate entry and spread, and are all important targets of neutralizing antibodies. Strains of HCMV vary considerably in the levels of gH/gL/gO and gH/gL/UL128-131 and this can impact infectivity and cell tropism. In this report, we investigated how natural interstrain variation in the amino acid sequence of gO influences the biology of HCMV. Heterologous gO recombinants were constructed in which 6 of the 8 alleles or genotypes (GT) of gO were analyzed in the backgrounds of strain TR and Merlin (ME). The levels of gH/gL complexes were not affected, but there were impacts on entry, spread and neutralization by anti-gH antibodies. AD169 (AD) gO (GT1a) drastically reduced cell-free infectivity of both strains on fibroblasts and epithelial cells. PHgO(GT2a) increased cell-free infectivity of TR in both cell types, but spread in fibroblasts was impaired. In contrast, spread of ME in both cell types was enhanced by Towne (TN) gO (GT4), despite similar cell-free infectivity. TR expressing TNgO(GT4) was resistant to neutralization by anti-gH antibodies AP86 and 14-4b, whereas ADgO(GT1a) conferred resistance to 14-4b, but enhanced neutralization by AP86. Conversely, ME expressing ADgO(GT1a) was more resistant to 14-4b. These results suggest; 1) mechanistically distinct roles for gH/gL/gO in cell-free and cell-to-cell spread, 2) gO isoforms can differentially shield the virus from neutralizing antibodies, and 3) effects of gO polymorphisms are epistatically dependent on other variable loci.

IMPORTANCE

Advances in HCMV population genetics have greatly outpaced understanding of the links between genetic diversity and phenotypic variation. Moreover, recombination between genotypes may shuffle diverse loci into various combinations with unknown outcomes. UL74(gO) is an important determinant of HCMV infectivity, and one of the most diverse loci in the viral genome. By analyzing interstrain heterologous UL74(gO) recombinants, we show that gO diversity can have dramatic impacts on cell-free and cell-to-cell spread as well as on antibody neutralization and that the manifestation of these impacts can be subject to epistatic influences of the global genetic background. These results offer a plausible explanation for the incomplete protection of the natural anti-HCMV antibody response.

INTRODUCTION

Recent application of state-of-the-art genomics approaches have begun to uncover a greater and more complex genetic diversity of human cytomegalovirus (HCMV) than had been appreciated (1–8). Of the 165 canonical open reading frames (ORFs) in the 235 kbp HCMV genome, 21 show particularly high nucleotide diversity and are distributed throughout the otherwise highly conserved genome. Links between specific genotypes and observed phenotypes are not well understood and as a corollary outcome, the factors driving HCMV genetic diversity and evolution remain speculative. This is further complicated by recombination between genotypes that can shuffle the diverse loci into various combinations, and this may result in epistasis where the phenotypic manifestation of a specific genotype of one locus may be influenced by the specific genotypes of other loci. Thus, realizing the full potential of modern genomics approaches towards the design of new interventions, clinical assessments and predictions will require better mechanistic understanding of the links between genotypes and phenotypes.

The UL74 ORF codes for glycoprotein (g) O and is one of the aforementioned highly diverse loci of HCMV (9) (10) (11) (12). Most phylogenetic groupings indicate 8 genotypes or alleles of gO that differ in 10-30% of amino acids, predominately near the N-terminus and in a short central region. These amino acid polymorphisms also affect predicted N-linked glycan sites. The evolutionary origins of gO genotype diversity are not understood. Studies that followed infected humans through latency-reactivation cycles over several years demonstrated remarkable stability in UL74(gO) sequences, arguing against the idea of selective pressure from a dynamically adapting host immune system as a driving force for gO diversity (11, 13). The functional significance of gO diversity has only recently been addressed and centers around its role as a subunit of the envelope glycoprotein complex gH/gL/gO, which is involved in the initiation of infection into different cell types.

The general model for herpesvirus entry involves fusion between the virion envelope and cell membranes mediated by the fusion protein gB and the regulatory protein gH/gL (14–16). The HCMV gH/gL can be unbound, or bound by gO or the set of UL128-131 proteins (17–20). How these gH/gL complexes participate to mediate infection is complicated and seems to depend on both the cell type and whether the infection is by cell-free virus or direct cell-to-cell spread. Efficient infection of all cultured cell types by cell-free HCMV is dependent on gH/gL/gO, whereas infection of select cell types including epithelial and endothelial

cells additionally requires gH/gL/UL128-131 (21–26). Experiments involving HCMV mutants lacking either gO or UL128-131 suggested that cell-to-cell spread in fibroblast cultures can be mediated by either gH/gL/gO or gH/gL/UL128-131, whereas in endothelial and epithelial cells gH/gL/UL128-131 is required, and it has remained unclear whether gH/gL/gO plays any role (23, 25, 27, 28). While it is clear that gH/gL/gO can bind to the cell surface protein PDGFRα via gO, and that gH/gL/UL128-131 can bind NRP2 and OR14I1 via UL128-131, the specific function(s) of these receptor engagements is unclear, but may include virion attachment, regulation of gB fusion activity, or activation of signal transduction pathways (29–31). In the case of gH/gL/gO, binding to PDGFRα activates signaling pathways, but these are not required for successful HCMV replication (28, 30, 32). Stegmann et al. showed that binding of a gO null HCMV to fibroblasts and endothelial cells was impaired, yet it is unclear whether this was due to lack of PDGFRα engagement. (33). Finally, Wu et al. reported coimmunoprecipitation of gB with gH/gL/gO and PDGFRα, consistent with a role for the gH/gL/gO-PDGFRα interaction in promoting gB fusion activity (32). However, unbound gH/gL has been shown to mediate cell-cell fusion and has also been found in stable complex with gB in extracts of infected cells and extracellular virions (20, 34). Thus, although many of the key factors in HCMV entry and cell-to-cell spread have been identified, their interplay in the various entry pathways is unclear. Moreover, the influence of gO diversity remains a mystery.

The gH/gL complexes have been extensively studied as potential vaccine candidates and neutralizing antibodies have been described that react with epitopes on gH/gL, on UL128-131 and on gO (35–43). Anti-UL128-131 antibodies neutralize with high potency, but only on cell types for which gH/gL/UL128-131 is required for entry; e.g., epithelial cells. In contrast, antibodies that react with epitopes on gH/gL tend to neutralize virus on both fibroblasts and epithelial cells, but are far less potent on fibroblasts, where only gH/gL/gO is needed for entry. One explanation for these observations is that gO, with its extensive N-linked glycan decorations presents more steric hindrance to the underlying gH/gL epitopes than do the UL128-131 proteins. Similar effects of glycans in shielding neutralizing epitopes have been described for HIV env, and for HCMV gN (44) (45). In support of this hypothesis for gO, Jiang et al. showed that focal spread of a gO null HCMV in fibroblasts was more sensitive to anti-gH antibodies (46). Recently, Cui et al. described antibodies that reacted to a linear epitope on gH that exhibited strain-selective neutralization that could not be explained

by polymorphisms within the gH epitope (47). One possible explanation was that gO polymorphisms between the strains imposed differential steric hindrances on these antibodies.

To gain more understanding for the functional implications of gO diversity we have utilized a set of HCMV BAC-clones as prototypes for phenotypic diversity. HCMV TB40/e (TB), TR and Merlin (ME) differ dramatically in the amounts of gH/gL complexes in the virion envelope and their infectivity on fibroblasts and epithelial cells. Extracellular virions of TB and TR contain gH/gL predominately in the form of gH/gL/gO and are far more infectious on both fibroblasts and epithelial cells than ME, which contains overall lower amounts of gH/gL, predominately as gH/gL/UL128-131 (9, 26). Each of these strains encodes a different representative of the 8 gO genotypes. In a previous report, we demonstrated that variation in the UL74(gO) ORF was not responsible for the observed differences between TR and ME. (48). Rather, it was shown that the amounts of gH/gL/gO in ME and TR virions were influenced by different steady-state levels of gO present during progeny assembly. Kalser et al. showed that replacing the gO of TB with that of Towne (TN) also did not affect the levels of gH/gL complexes but may have enhanced the ability of TB to spread in epithelial cell cultures (49). Here, we have generated a set of heterologous gO recombinants to include 6 of the 8 genotypes in the genetic backgrounds of the gH/gL/gO-rich strain TR and the gH/gL/UL128-131-rich ME to analyze how the differences in gO sequence influence HCMV biology. The results demonstrate that gO variation can have dramatic effects on cell-free entry, cell-to-cell spread and the neutralization by anti-gH antibodies. In some cases opposite influences were observed for a given gO genotype in the different backgrounds of TR and ME, indicating epistasis with other genetic differences between these strains.

RESULTS

Influences of gO polymorphisms on cell-free infectivity and tropism can be dependent on the background strain. To examine the effects of gO polymorphism, a set of recombinant viruses was constructed in which the endogenous UL74(gO) ORFs of strain TR and ME were replaced with the UL74(gO) ORFs from 5 other strains. BAC-cloned strains TR and ME were chosen as the backgrounds for these studies since they represent gH/gL/gO-rich and gH/gL/UL128-131-rich strains respectively (9, 26, 49). Additionally, ME is restricted to a cell-to-cell mode of spread in culture, whereas TR is capable of both cell-free and cell-to-cell modes of spread (23, 50, 51). The intended changes to UL74(gO) in each recombinant BAC were verified

145 by sequencing the UL74 ORF and the flanking regions used for BAC recombineering. However, it was
146 recently reported that HCMV BAC-clones can sustain various genetic deletions, and rearrangements, and
147 mutations during rescue in fibroblasts or epithelial cells, resulting in mixed genotype populations (52). To
148 ensure that phenotypes characterized were the associated with the intended changes to UL74(gO) and not to
149 other genetic changes sustained during BAC rescue in fibroblasts, all analyses were performed on at least
150 three independently BAC-rescued viral stocks.

151 As a basis for interpretation of the later biological comparisons among recombinants, the levels of
152 gH/gL complexes incorporated into the virion envelope were analyzed by immunoblot as previously described
153 (9, 26). As in the previous reports, TR contained predominantly gH/gL/gO, whereas ME contained mostly
154 gH/gL/UL128-131 (Fig 1, compare lane 1 in panels A and B). Propagation of ME under conditions of UL131
155 transcriptional repression (denoted "Merlin-T" (MT) as described (26, 51)), resulted in more gH/gL/gO and less
156 gH/gL/UL128-131 (Fig. 1C, lane 1). Some minor differences in the amounts of total gL, gH/gL/gO, and
157 gH/gL/UL128-131 were observed for some of the heterologous gO recombinants relative to their parental
158 strains. However, band density analyses showed that all apparent differences were less than 3-fold and few
159 reached statistical significance when compared across multiple experiments, likely reflecting the limitations of
160 immunoblot as a precise quantitative method, as well as stock-to-stock variability in glycoprotein composition
161 (Table 1). Thus, consistent with our previous report, differences between strains TR and ME in the
162 abundance of gH/gL complexes are predominately influenced by genetic background differences outside the
163 UL74(gO) ORF (48).

164 While gH/gL/gO is clearly important for entry into both fibroblasts and epithelial cells, the mechanisms
165 are likely different since 1) fibroblasts clearly express the gH/gL/gO receptor PDGFRα on their surface,
166 whereas ARPE19 epithelial cells express little or none of this protein (28, 30, 32, 53), and 2) entry into
167 epithelial cells requires gH/gL/UL128-131 in addition to gH/gL/gO (23, 24, 26). Thus, it was possible that gO
168 polymorphisms would differentially affect replication in these two cell types. To address this, fibroblast-to-
169 epithelial tropism ratios were determined for each parental strain and gO recombinant by inoculating cultures of
170 fibroblasts and epithelial cells in parallel with equivalent amounts of cell-free virus stocks. The number of
171 infected cells in each culture was then determined by flow cytometry using GFP expressed from the virus
172 genome. Figure 2 shows the results of these experiments as the fold preference for either cell type as a ratio,

173 where “1” indicates equal infection of both cell types. Stocks of the parental TR were approximately 20-fold
174 more infectious on fibroblasts than on epithelial cells (Fig 2A). Preference towards fibroblasts was greater for
175 TR-recombinants expressing MEgO(GT5), PHgO(GT2b), and TBgO(GT1c). In contrast, tropism ratios of TR-
176 recombinants expressing ADgO(GT1a) and TNgO(GT4) were closer to 1, indicating more equal infection of
177 both cell types. Parental ME and all of the ME-based gO recombinants had tropism ratios within the range of 6
178 in favor of fibroblasts to 3 in favor of epithelial cells. Several of these viruses had variability between replicate
179 stocks where some had slight fibroblasts preference and others slight epithelial preference (Fig 2B).
180 Propagation of the ME-based viruses as MT greatly increased the preference towards fibroblasts infection for
181 all recombinants to a range of 30-300 fold (Fig 2B). These results suggested that for the more gH/gL/gO-rich
182 TR and MT, gO polymorphisms may differentially influence the infection of fibroblasts and epithelial cells,
183 shifting the apparent relative tropism. However, such influences were less pronounced for ME, consistent with
184 the low abundance of gH/gL/gO expressed by this virus.

185 It was not clear if the observed differences in tropism ratios were due to enhanced infection of one cell
186 type, reduced infection of the other cell type or a mixture of both. To address this, specific infectivity (ratio of
187 the number of virions to the number of infectious units) was determined for each parental and recombinant on
188 both fibroblasts and epithelial cells. Multiple independent supernatant stocks of each recombinant were
189 analyzed by qPCR for encapsidated viral genomes and infectious titers on both cell types were determined by
190 flow cytometry quantification of GFP-positive cells (Fig 3). For the TR-based viruses on fibroblasts,
191 MEgO(GT5), TBgO(GT1c), and TNgO(GT4) each resulted in moderately enhanced infectivity (2 to 10-fold
192 fewer genomes/IU) compared to the parental TR, and PHgO(GT2a) enhanced infectivity 30-fold. In contrast,
193 ADgO(GT1a) reduced TR infectivity by 90-fold (Fig 3A, top panel). In our previous report, expression of MEgO
194 in the TR background did not appear to affect infectivity on fibroblasts (48). This discrepancy was likely due to
195 the more sensitive flow cytometry readout used in the current studies as compared to the plaque assay
196 readout used previously. The infectivity of parental TR on epithelial cells was about 20-fold lower than on
197 fibroblasts (i.e., 20-fold higher genomes/IU), but the relative effect of each heterologous gO was similar to that
198 observed on fibroblasts (Fig 3A, bottom panel). Thus, some of the gO changes had dramatic effects on the
199 infectivity of TR. Although these effects were manifest on both cell types, they were more pronounced on
200 fibroblasts and this explains the observed differences in fibroblast preferences reported in Figure 2A.

Cell-free ME virions were very poorly infectious on both cell types, with specific infectivity values of greater than 1 x 10^6 genomes/IU (Fig 3B). Changes to the UL74(gO) ORF did not significantly affect the infectivity on either cell type except in the case of ADgO(GT1a), which further reduced epithelial infectivity. When propagated as MT, infectivity on both cell types was improved to levels comparable to TR and this was consistent with our previous results (Fig 2C) (26, 48). Unlike TR, where most of the heterologous gO recombinants influenced infectivity, fewer of the gO isoforms resulted in significant alteration of infectivity in the context of MT. ADgO(GT1a) reduced MT infectivity on both cell types, TNgO(GT4) moderately enhanced infectivity on epithelial cells and TBgO(GT1c) slightly decreased infectivity on epithelial cells. Thus, as in the TR background, some changes to gO influenced infectivity of MT and this was disproportionally manifest on fibroblasts compared epithelial cells, but the overall preference of all of the MT-based viruses was strongly in favor of fibroblasts. In contrast, gO changes had little effect on the infectivity or tropism of ME-based viruses. Together with the finding that ME specific infectivity was greater than 10^6 genomes/IU, and the results of Laib Sampaio {Laib Sampaio et al., 2016, #46364} who showed that deletion of UL74(gO) from ME had no detectible phenotype, the lack of effect of gO polymorphism suggests that the low efficiency infection of ME reflects a gH/gL/gO independent mechanism.

It has been reported that gO-null HCMV are impaired for attachment to cells and that soluble gH/gL/gO can block HCMV attachment (33, 54). Thus, it was possible that the observed changes to cell-free infectivity due to gO polymorphisms were related to a role for gO in attachment. To test this hypothesis, each heterologous gO recombinant was compared to the corresponding parental strain by applying cell-free virus stocks to fibroblast or epithelial cell cultures for approximately 20 min, washing away the unbound virus and then counting the numbers of cell-associated virions by immunofluorescence staining of the capsid-associated tegument protein pp150 (33) (Fig 4 and Tables 2 and 3). The input concentrations for each experiment were determined empirically to give sufficient bound virus for quantitation, and be equal for each set parental and heterologous gO recombinants within the constraints of the stock titers. The average number of cell-associated virions per cell varied considerable between experiments, likely reflecting the complex parameters expected to influence virus attachment including stock concentration, cell state and variability in the incubation time between experiments. In some cases, a given recombinant was significantly different from parental in only one or two of the three experiments. In other cases recombinants were significantly different from parental

229 in all three experiments but the differences varied in being greater than or less than. Both of these cases
230 suggested that these specific gO isoforms did not affect binding or attachment of HCMV to cells. However,
231 TR_TNgO(GT4), ME_ADgO(GT1a) and MT_ADgO(GT1a) were each significantly lower than their respective
232 parental viruses in all three experiments on both fibroblasts and epithelial cells. While it was possible that the
233 reduced binding of MT_ADgO(GT1a) was due in part to the slightly lower amounts of gH/gL/gO (Fig 1C and
234 Table 1), the reduced binding of TR_TNgO(GT4) could not be similarly explained since this virus had slightly
235 more gH/gL/gO than the parental TR (Fig. 1A, Table 1). Moreover, reduced binding may help explain the lower
236 infectivity of ME_ADgO(GT1a) (Fig 3C), but the poor infectivity of TR_ADgO(GT1a) could not be explained by
237 poor binding, and the reduced binding of TR_TNgO(GT4) did not result in reduction of infectivity (Fig 3A).

238 In sum, these analyses indicated that; 1) gO polymorphisms can influence the cell-free infectivity of
239 HCMV. In some cases this was independent of any effects on abundance of gH/gL/gO in the virion envelope
240 or binding to cells (e.g. parental TR and TR recombinants harboring MEgO(GT5), TBgO(GT1c), and
241 ADgO(GT1a), had dramatically different infectivity but comparable levels of gH/gL/gO and cell binding). 2) The
242 influence of some gO isoforms was dependent on the background strain (e.g., PHgO(GT2a) enhanced TR
243 infectivity but did not affect ME or MT and TNgO(GT4) reduced binding of TR but has no effect on binding of
244 ME or MT). 3) While some heterologous gO recombinants had quantitatively different effects on infectivity on
245 fibroblast compared to epithelial cells, these did not change the fundamental fibroblast preferences for either
246 TR or MT. 4) Some of the heterologous gO recombinants did appear to change relative tropism of ME.
247 However, the relevance of tropism ratios for these viruses is questionable since the specific infectivity values
248 for all ME-based recombinants were greater then $1x10^6$ genomes/IU, suggesting that the cell-free virions of ME
249 were essentially noninfectious on either cell type. This was consistent with the highly cell-associated nature of
250 ME (50, 51).

251 **Polymorphisms in gO can differentially influence the mechanisms of cell-free and cell-to-cell**
252 **spread.** The analyses described above focused on the cell-free infectivity of HCMV, as indicative of a cell-free
253 mode of spread. Cell-to-cell spread mechanisms are likely important for HCMV, and while gH/gL complexes
254 are clearly important for cell-to-cell spread, the mechanisms in these processes are poorly characterized in
255 comparison to cell-free infection. Strains TR and ME are well-suited to compare the effects of gO
256 polymorphisms on cell-free and cell-to-cell spread since ME is essentially restricted to cell-to-cell due to the

poor infectivity of cell-free virions but can be allowed to also spread cell-free by propagation as MT, whereas TR can spread by both cell-free and cell-to-cell mechanisms (23, 26, 50, 51).

To compare spread among heterologous gO recombinants, replicate cultures were infected at low multiplicity, and at 12 dpi, foci morphology was documented by fluorescence microscopy and the increased number of infected cells was determined by flow cytometry. In fibroblasts cultures, parental TR and MT showed more diffuse foci compared to the tight, localized focal pattern of parental ME, consistent with the notion that TR and MT spread by both cell-free and cell-to-cell mechanisms whereas ME was restricted to cell-to-cell spread (Fig 5A). Quantitatively, spread by parental TR increased the numbers of infected cells 55-fold over 12 days, whereas spread of TR_MEgO(GT5) and TR_PHgO(GT2a) were significantly reduced (Fig 5B). Spread of ME was slightly reduced by ADgO(GT1a), but was increased by TNgO(GT4) (Fig 5C). Surprisingly, different effects on spread were observed for MT where TBgO(GT1c) and TNgO(GT4) reduced spread, and ADgO(GT1a) increased spread.

A number of interesting incongruities were observed when comparing the cell-free infectivity of some gO recombinants on fibroblasts to their respective spread characteristics in fibroblasts; 1) Spread of TR_PHgO in fibroblasts was reduced compared to the parental TR (Fig 5B), but the cell-free infectivity of this recombinant was actually better (Fig 3A). Similarly, spread of both MT_TBgO(GT1c) and MT_TNgO(GT4) were reduced in fibroblasts (Fig 5D), but cell-free infectivity of both viruses was comparable to parental MT. 2) Conversely, MT_ADgO(GT1a) spread better in fibroblasts (Fig 5D), but the cell-free infectivity was substantially worse (Fig 3C). Since the efficiency of cell-free spread should depend on both the specific infectivity and the quantities of progeny virus released to the culture supernatants, it was possible that some of these incongruities reflected offsetting differences in the quantity of cell-free virus released as compared to their infectivity. To test this, fibroblasts cultures were infected at MOI 1 and after 8 days, released progeny were quantified by qPCR for viral genomes in the culture supernatants. There were no significant differences in the quantity of progeny released per cell for any of the TR or ME-based recombinants (Fig. 6A, and B). Likewise, all of MT-based recombinants released similar numbers of cell-free progeny except for MT_ADgO(GT1a), which was reduced by approximately 4-fold (Fig. 6C). Thus, the discrepancies between efficiency of spread and cell-free infectivity could not be explained by offsetting differences in the release of cell-free progeny. Rather, these results suggested that gO polymorphisms can differentially influence the mechanisms of cell-free and cell-to-cell

spread in fibroblasts. The interpretation that gH/gL/gO can provide a specific function for cell-to-cell spread was supported by the results that expression of ADgO(GT1a) and TNgO(GT4), respectively reduced and increased spread of the strain ME, a strain known to spread predominantly cell-to-cell (Fig 5C).

Spread was also analyzed in epithelial cell cultures. Here, foci of both TR and ME remained tightly localized, suggesting predominantly cell-to-cell modes of spread for both strains in this cell type (Fig. 7A). The number of TR-infected cells increased by only 5-6 fold over 12 days compared to approximately 25-fold for ME (Fig 7B and C). The low efficiency of spread for TR in epithelial cells compared to ME was documented previously and may relate to the low expression of gH/gL/UL128-131 by TR compared to ME (23, 26, 55). Expression of TNgO(GT4) further reduced TR spread in epithelial cells (Fig 7B). In contrast, ME spread was slightly reduced by TBgO(GT1c) and ADgO(GT1a), but nearly doubled by TNgO(GT4). Note that spread of MT could not be addressed in epithelial cells, since gH/gL/UL128-131 is clearly required for spread in these cells and its repression would complicate analysis of the contribution of gO polymorphism (23). Nevertheless, it is clear from these experiments that gO polymorphisms can affect spread in epithelial cells and that this can depend on the background strain. Specifically, TNgO(GT4) reduced TR spread but increased ME spread. This suggested that although gH/gL/UL128-131 is required for efficient cell-to-cell spread in epithelial cells, and may even be sufficient for spread, gH/gL/gO also contributes to the mechanism when present.

Polymorphisms in gO can affect antibody neutralization on gH epitopes. The extensive N-linked glycosylation of gO raised the possibility that gO could present steric hindrance to the binding of antibodies to epitopes on gH/gL, as was shown for HCMV gN and also HIV env (44, 45). A corollary hypothesis was that such effects might vary with the polymorphism among gO isoforms. To address this, neutralization experiments were conducted using two monoclonal anti-gH antibodies; 14-4b, which recognizes a discontinuous epitope likely located near the membrane proximal ectodomain of gH (35, 56) and AP86, which binds to a continuous epitope near the N-terminus of gH (57). Note that these experiments could only be performed with TR- and MT-based recombinants since the cell-free progeny of ME-based viruses were found to be only marginally infectious (Fig 3B).

Parental TR and recombinants encoding MEgO(GT5), PHgO(GT2a) and TBgO(GT1c) were completely neutralized on fibroblasts by mAb 14-4b, whereas TR_ADgO(GT1a) and TR_TNgO(GT4) were significantly resistant (Fig 8A). There was more variability among TR-based recombinants with mAb AP86 (Fig

313 8B). Here, parental TR could only be neutralized to approximately 40% residual infection. TNgO(GT4)
314 rendered TR totally resistant to mAb AP86, and MEgO(GT5) also significantly protected TR. In contrast,
315 TR_TBgO(GT1c) and TR_ADgO(GT1a) were more sensitive to mAb AP86. On epithelial cells neutralization
316 by both antibodies was more potent and complete than on fibroblasts, and there was less variability among gO
317 recombinants (Fig 8C, and D). This was consistent with the interpretation that both 14-4b and AP86 could bind
318 their epitopes on gH/gL/UL128-131 and that this represented the majority of the observed neutralization on
319 epithelial cells. However, TR_TNgO(GT4) still displayed some reduced sensitivity to both antibodies,
320 suggesting that gH/gL/gO epitopes also contributed to neutralization on epithelial cells.

321 MT-based recombinants were generally more sensitive to neutralization by 14-4b than were TR-based
322 viruses (compare 14-4b concentrations in Fig 8A and 9A). Strikingly, whereas TNgO(GT4) conferred 14-4b
323 resistance to TR, it did not in MT, and instead ADgO(GT1a) provided resistance to 14-4b (Fig 9A). As was
324 observed for TR-based recombinants, 14-4b neutralization on epithelial cells was less affected by gO
325 polymorphisms (Fig 9B). Note that neutralization of MT-based recombinants by AP86 could not be tested
326 since MEgH harbors a polymorphism in the linear AP86 epitope that precludes reactivity (57). Together, these
327 results indicated that differences among gO genotypes can differentially affect antibody neutralization on gH
328 epitopes. Moreover, which gO genotype could protect against which antibody depended on the background
329 strain, suggesting the combined effects of gO polymorphisms and gH/gL polymorphisms.

330 **DISCUSSION**

331 Efficient cell-free infection of most, if not all cell types requires gH/gL/gO (22, 25, 26). However, the
332 details of the mechanisms, and the distinctions between the roles of gH/gL/gO in cell-free and cell-to-cell
333 spread remain to be clarified. While there are naturally occurring amino acid polymorphisms in each subunit of
334 gH/gL/gO, gO has the most dramatic variation, with 8 known genotypes (or alleles) that differ between 10-30%
335 of amino acids (9–12). All isoforms of gO are predicted to have extensive N-linked glycan modifications and
336 some of the amino acid differences alter the predicted sites. In a previous report, we sought to determine if gO
337 polymorphisms were a factor influencing the different levels of gH/gL/gO and gH/gL/UL128-131 in strains TR
338 and ME. On the contrary, results suggested that genetic differences outside the UL74(gO) ORF result in more
339 rapid degradation of gO in the ME-infected cells compared to TR, and this influences the pool of gO available
340 during progeny assembly (48). Kalser et al. reported that gO polymorphism could differentially affect multi-step

341 replication kinetics in fibroblasts and epithelial cells (49). However, only TB was analyzed as the background
342 and distinctions between effects on cell-free and cell-to-cell spread were unclear. In this report we constructed
343 a matched set of heterologous gO recombinants in the well-characterized, BAC-cloned strains TR and ME.
344 Studies included address aspects of cell-free and cell-to-cell spread, cell-type tropism and neutralization by
345 anti-gH antibodies. The results demonstrate that gO polymorphisms can influence each of these parameters
346 and the effects in some cases were dependent on the genetic background, suggesting a number of possible
347 epistatic phenomena at play.

348 A commonly used measure to assess the tropism of HCMV strains, isolates and recombinants is the
349 ratio of infection between fibroblasts and other cell types, including epithelial and endothelial cells (49, 55, 58,
350 59). Expressions of this ratio have varied, but have generally involved a normalization of the epithelial or
351 endothelial infection to that of fibroblasts. Here we similarly determined the infection titer of each of the
352 parental strains and heterologous gO recombinants on both fibroblasts and epithelial cells and expressed
353 ratios ≥1 (either fibroblasts/epithelial or epithelial/fibroblasts) to indicate the fold cell type preference or tropism
354 of each virus (Fig 2). Both gH/gL/gO-rich viruses, TR and MT, were strongly fibroblast-tropic and some
355 heterologous gO isoforms enhanced this preference or while others reduced it. In contrast, the gH/gL/UL128-
356 131-rich virus ME infected both cell type more equally (ratios closer to 1), and gO polymorphisms had little
357 effect. The limitation of any such measure of relative tropism is that it does not determine whether the virus in
358 question can efficiently infect one cell type in particular, both or neither. Thus, any 2 viruses compared may
359 have the same fibroblast-to-epithelial cell infectivity ratio for completely different reasons. To address this we
360 also compared infectivity on both cell types using a common comparison for all viruses, i.e., the number of
361 virions in the stock as determined by qPCR for DNAse-protected viral genomes in the cell-free virus stocks (Fig
362 3). This analysis provided a measure of specific infectivity as the number of genomes/IU, where the lower ratio
363 indicates more efficient infection. Whether higher genomes/IU values reflect the presence of greater numbers
364 of *bona fide* "defective" virions, or a lower probability or efficiency of each viable virion in the stock to
365 accomplish a detectable infection, and whether or how these two possibilities are different is difficult to know
366 for any type of virus. Nevertheless, these analyses provided important insights to the tropism ratios reported.
367 In general, the specific infectivity of the gH/gL/gO-rich viruses TR and MT in these experiments were in the
368 range of 500-5000 genomes/IU on fibroblasts and were approximately 20-100 fold higher on epithelial cells,

369 explaining the strong fibroblast preference exhibited by these strains. The effect of most heterologous gO
370 isoforms was reciprocal on both cell types, but often of larger magnitude on fibroblasts. Thus, while all of the
371 TR and MT-based gO recombinants remained fibroblast tropic, the quantitatively different effects on the two
372 cell types influenced the magnitude of fibroblasts preference. Importantly, in no case did the change of gO
373 affect the fundamental fibroblast preference of either TR or MT. Specific infectivity of the gH/gL/UL128-131-
374 rich, ME-based viruses were all over 10^6 genomes/IU, on both cell types. These values indicate very low
375 infectivity of the cell-free virions, consistent with the described cell-associated spread nature of ME (27, 50, 51,
376 55). Changes to gO had little or no effect except in the case of ADgO(GT1a), which further reduced the
377 infectivity of ME on epithelial cells. These results indicate that the low infectivity of ME virions is related to the
378 low level of gH/gL/gO complex, not the specific isoform of gO involved. Moreover, viewed in light of specific
379 infectivity analyses, the near neutral fibroblast-to-epithelial tropism ratios of the ME-based viruses seem to
380 reflect an equal inability to infect either cell type and thus any assertion of a "preference" for either cell type for
381 any of these viruses seems spurious.

382 Binding to PDGFRα through gO is clearly critical for infection of fibroblasts (30). However, while
383 gH/gL/gO is also important for infection of epithelial cells, the literature is conflicted on the expression of
384 PDGFRα and its importance for HCMV infection in epithelial and endothelial cells (26, 28, 29, 32, 33). On
385 either cell type, possible mechanisms of gH/gL/gO include facilitating initial attachment to cells, promoting gB-
386 mediated membrane fusion, and signaling though PDGFRα or other receptors. While Wu et al. were able to
387 coimmunoprecipitate gB with gH/gL/gO and PDGFRα, Vanarsdall et al. showed that gH/gL without gO or
388 UL128-131 can directly interact with gB and promote gB-fusion activity (20, 32, 34). It has also been shown
389 that gH/gL/gO engagement of PDFGRα can elicit signaling cascades, but that this is not required for infection
390 (28, 30, 32). In contrast, there is evidence that gH/gL/gO can help facilitate initial virion attachment (33, 54). In
391 our studies, TNgO(GT4) reduced binding of TR to both fibroblasts and epithelial cells (Fig 4, Tables 2 and 3).
392 However, the reduced binding of TR_TNgO(GT4) did not result in reduced infection on either cell type, and
393 there were other isoforms of gO that either resulted in increased or decreased infectivity but were not
394 associated with any detectable alteration in binding. Thus, while gH/gL/gO may contribute to initial binding, it is
395 likely involved in other important mechanisms that facilitate infection and these can be influenced by gO
396 polymorphisms. For example, is possible that polymorphisms in gO can affect the nature and outcome of

397 PDGFRα engagement. In support of this hypothesis, Stegmann et al. showed that mutation of conserved
398 residues within the N-terminal variable domain of gO were critical for PDGFRα binding (60). Thus it is
399 conceivable that the variable residues of gO can alter the architecture of the interaction with PDGFRα.
400 Alternatively, it may be that there are other receptors on both cell types for gH/gL/gO and that gO
401 polymorphisms can affect those interactions. Also, the effects of several specific gO isoforms observed in the
402 TR-background were not observed in the ME or MT-backgrounds. Possible explanations for the apparent
403 epistasis include not only the differential contributions of polymorphisms in gH/gL, but also potential differences
404 between strains in other envelope glycoproteins, such as gB, or gM/gN may influence the relative importance
405 of gH/gL/gO for binding and infection.

406 The mechanistic distinctions between cell-free and cell-to-cell spread of HCMV are unclear. Spread of
407 ME in both fibroblast, epithelial and endothelial cells is almost exclusively cell-to-cell and this can be at least
408 partially explained by the low infectivity of cell-free ME virions (Fig 3; specific infectivity > 10^6 genomes/IU) (27,
409 50, 51, 55). Laib Sampaio et al. showed that inactivation of the UL74(gO)ORF in ME did not impair spread but
410 that a dual inactivation of both gO and UL128 completely abrogated spread (27). This indicates that
411 gH/gL/UL128-131 is sufficient for cell-to-cell spread in fibroblasts or endothelial cells in the absence of
412 gH/gL/gO, and it seems likely that spread in epithelial cells might be similar in this respect. Our finding that
413 various heterologous gO isoforms can enhance or reduce spread of ME without affecting the cell-free infectivity
414 strongly suggest that while gH/gL/UL128-131 may be sufficient for cell-to-cell spread, gH/gL/gO can modulate
415 or mediate the process, if present in sufficient amounts. In the context of MT, where expression of
416 gH/gL/UL128-131 is reduced to sub-detectable levels (26, 51) the virus gained cell-free spread capability, and
417 yet some of the heterologous gO isoforms had opposite effects on cell-free infectivity and spread (compare Fig
418 3C to 5D). Similar discorrelations between cell-free infectivity and spread were observed for the naturally
419 gH/gL/gO-rich strain TR, albeit with different heterologous gO isoforms involved. That gO polymorphisms can
420 have opposite effects on cell-free and cell-to-cell spread supports a hypothesis of mechanistic differences in
421 how gH/gL/gO mediates the two processes, and again these effects seem dependent on episatic influences of
422 the different genetic backgrounds.

423 Beyond the roles of gH/gL/gO in replication, the complex is likely a significant target of neutralizing
424 antibodies, and therefore a valid candidate for vaccine design. Several groups have reported neutralizing

antibodies that react with epitopes contained on the gH/gL base of both gH/gL/UL128-131 and gH/gL/gO and others that react to on gO (35–43). We found that changing the gO isoform can have dramatic effects on the sensitivity to two anti-gH mAbs (Figs 8 and 9). In the TR background on fibroblasts, both ADgO(GT1a) and TNgO(GT4) conferred significant resistance to neutralization by 14-4b, which likely reacts to a discontinuous epitope near the membrane proximal ectodomain of gH (35, 56). TNgO(GT4) also conferred resistance to AP86, which reacts to a linear epitope near the N-terminus of gH (57), whereas ADgO(GT1a) actually increased sensitivity of TR to AP86. Neutralization by either antibody on epithelial cells was not significantly affected, consistent with the notion that these antibodies can also neutralize in the context of gH/gL/UL128-131. Again, the strain background exerted considerable influence over the effects of gO polymorphisms. For MT, it was ADgO(GT1a) that conferred resistance to 14-4b, and the other isoforms had little or no effect. Here it is important to note that gH of ME and TR fall into distinct genotype families, which in part affect the N-terminus including the AP86 epitope, such that the antibody reacts with TRgH but not ME (or MT) gH (10, 57). The observed effects on neutralization on gH epitopes likely involve differences in how gO variable regions or associated glycans fold onto gH/gL to exert differential steric effects. Relatedly, the differential influence of gO isoforms in the two genetic backgrounds suggests epistasis involving the additive effects of gO polymorphisms with the more subtle gH polymorphisms, which together can differentially affect the global conformation of the gH/gL/gO trimer.

In conclusion, we have shown that naturally occurring polymorphisms in the HCMV gO can have a dramatic influence on significant aspects of HCMV biology including, cell-free and cell-to-cell spread, and neutralization by anti-gH antibodies. These effects could not be explained by changes to the levels of gH/gL complexes in the virion envelope, but rather point to changes in the mechanism(s) of gH/gL/gO in the processes of cell-free and cell-to-cell spread. The associated epistasis with the global genetic background highlights a particular challenge for intervention approaches since humans can be superinfected with several combinations of HCMV genotypes and recombination may occur frequently (1–8). Moreover, these observations could help explain the incomplete protection observed for the natural antibody response against HCMV.

MATERIALS AND METHODS

Cell lines. Primary neonatal human dermal fibroblasts (nHDF; Thermo Fisher Scientific), MRC-5 fibroblasts (ATCC CCL-171; American Type Culture Collection), and HFFFtet cells (which express the tetracycline [Tet] repressor protein; provided by Richard Stanton) {Stanton et al., 2010, #13634} were grown in Dulbecco's modified Eagle's medium (DMEM; Thermo Fisher Scientific) supplemented with 6% heat-inactivated fetal bovine serum (FBS; Rocky Mountain Biologicals, Inc., Missoula, MT, USA) and 6% bovine growth serum (BGS; Rocky Mountain Biologicals, Inc., Missoula, MT, USA) and and with penicillin streptomycin, gentamycin and amphotericin B. Retinal pigment epithelial cells (ARPE19) (American Type Culture Collection, Manassas, VA, USA) were grown in a 1:1 mixture of DMEM and Ham's F-12 medium (DMEM:F-12)(Gibco) and supplemented with 10% FBS and with penicillin streptomycin, gentamycin and amphotericin B.

Human Cytomegalovirus (HCMV). All HCMV were derived from bacterial artificial chromosome (BAC) clones. The BAC clone of TR was provided by Jay Nelson (Oregon Health and Sciences University, Portland, OR, USA) (61). The BAC clone of Merlin (ME) (pAL1393), which carries tetracycline operator sequences in the transcriptional promoter of UL130 and UL131, was provided by Richard Stanton (51). All BAC clones were modified to express green fluorescent protein (GFP) by replacing the US11 ORF with the eGFP gene under the control of the murine CMV major immediate early promoter. The constitutive expression of eGFP allows the monitoring of HCMV infection early and was strain-independent. Infectious HCMV was recovered by electroporation of BAC DNA into MRC-5 fibroblasts, as described previously by Wille et al. (25) and then coculturing with nHDF or HFFFtet cells. Cell-free HCMV stocks were produced by infecting HFF or HFFFtet cells at 2 PFU per cell and harvesting culture supernatants at 8 to 10 days postinfection (when cells were still visually intact). Harvested culture supernatants were clarified by centrifugation at 1,000 X g for 15 min. Stock aliquots were stored at -80°C. Freeze-thaw cycles were avoided. Infectious unit (IU) were determined by infecting replicate cultures of nHDF or ARPE19 with serial 10-fold dilutions and using flow cytometry to count GFP positive cells at 48 hours post infection.

Heterologous UL74(gO) recombinant HCMV. A modified, three step BAC En Passant recombineering technique was performed (62, 63). In the first step, the endogenous UL74 ORF from the start codon to the stop codon of both TR and ME was replaced by a selectable marker. This necessary step was

480 added to prevent formation of chimeric UL74 gene by internal recombination of the UL74 BAC sequence and
481 the incoming heterologous UL74 ORF. A purified PCR product containing the ampicillin resistance selectable
482 marker (AmpR) cassette from the pUC18 plasmid flanked by sequences homologous to 50 bp upstream and
483 downstream of the TR or ME UL74 ORF was electroporated into the bacteria, recombination was induced and
484 the recombinant-positive bacteria were selected on medium containing ampicillin (50 µg/ml) and
485 chloramphenicol (12.5 µg/ml). The primers used to produce the TR- and ME-specific AmpR PCR bands are
486 For74TRamp, 5'-
487 CATGGGAGCTTTTTGTATCGTATTACGACATTGCTGTTTCCAGAACTTTAcgcggaacccctatttgtttatttttctaaatac,
488 For74MEamp, 5'-
489 GATGGGAGCTTTTTGTATCGTATTACGACATTGCTGCTTCCAGAACTTTAcgcggaacccctatttgtttatttttctaaatac,
490 and Rev74amp (used for both TR and ME PCR reactions), 5'-
491 CCAAACCACAAGGCAGACGGACGGTGCGGGGTCTCCTCCTCTGTCATGGGGttaccaatgcttaatcagtgaggcacc
492 . The lower case nucleotides correspond to the AmpR gene from the pUC18 plasmid, the upper case
493 nucleotides to the TR and ME BAC sequences immediately upstream and downstream of the UL74 ORF.
494 In the second step, the AmpR cassette in the TR and ME first-step intermediate BACs was replaced
495 with the UL74(gO) sequence from the heterologous strain containing the En Passant cassette (62, 63). Briefly,
496 E. coli cultures were prepared for recombination as described above for step 1 and electroporated with purified
497 PCR products containing the UL74 ORF from the TR or ME strain flanked by sequence homologous to 50 bp
498 upstream and downstream of the opposite strain. The UL74 ORF also contained an inserted En Passant
499 cassette (an I-SceI site followed by a kanamycin resistance gene surrounded by a 50-bp duplication of the
500 UL74 nucleotides of the insertion site). Transformed E. coli cells were induced for recombination and then
501 selected for the swap of the UL74 En Passant sequence into the BAC by growth on medium containing
502 kanamycin (50 µg/ml) and chloramphenicol (12.5 µg/ml). A PCR reaction analysis with primers located
503 upstream and downstream of UL74 was used to confirm the swap of the AmpR cassette by the En Passant
504 cassette/UL74 gene.
505 In the third step, several sequencing validated colonies of the second step were subjected to the last
506 step of the En Passant recombineering, that is, an induction of both the I-SceI endonuclease and the
507 recombinase {Tischer et al., 2006, #74288; Tischer et al., 2010, #13552}. The activity of these enzymes lead to

508 an intramolecular recombination in the UL74 sequence around the En Passant cassette and thus the
509 restoration of an uninterrupted, full length UL74 ORF. The final heterologous UL74(gO) recombinants were
510 verified by Sanger sequencing of PCR products using primers located upstream and downstream of the UL74
511 gene.

512 **Antibodies.** Monoclonal antibodies (MAbs) specific to HCMV major capsid protein (MCP), pp150, and
513 gH (14-4b and AP86) were provided by Bill Britt (University of Alabama, Birmingham, AL) (35, 57, 64, 65). 14-
514 4b and AP86 were purified by FPLC and quantified by the University of Montana Integrated Structural Biology
515 Core Facility. Rabbit polyclonal sera against HCMV gL was described previously (9, 26).

516 **Immunoblotting.** HCMV cell-free virions were solubilized in 2% SDS–20 mM Tris-buffered saline
517 (TBS) (pH 6.8). Insoluble material was cleared by centrifugation at 16,000 X g for 15min, and extracts were
518 then boiled for 10 min. For reducing blots, dithiothreitol (DTT) was added to extracts to a final concentration of
519 25 mM. After separation by SDS-PAGE, proteins were transferred onto polyvinylidene difluoride (PVDF)
520 membranes (Whatman) in a buffer containing 10 mM $NaHCO_3$ and 3mM Na_2CO_3 (pH 9.9) plus 10% methanol.
521 Transferred proteins were probed with MAbs or rabbit polyclonal antibodies, anti-rabbit or anti-mouse
522 secondary antibodies conjugated with horseradish peroxidase (Sigma-Aldrich), and Pierce ECL-Western
523 blotting substrate (Thermo Fisher Scientific). Chemiluminescence was detected using a Bio-Rad ChemiDoc
524 MP imaging system. Band densities were quantified using BioRad Image Lab v 5.1.

525 **Quantitative PCR.** Viral genomes were determined as described previously (26). Briefly, cell-free
526 HCMV stocks were treated with DNase I before extraction of viral genomic DNA (PureLink viral RNA/DNA
527 minikit; Life Technologies/Thermo Fisher Scientific). Primers specific for sequences within UL83 were used
528 with the MyiQ real-time PCR detection system (Bio-Rad).

529 **Flow cytometry.** Recombinant GFP-expressing HCMV-infected cells were washed twice with PBS
530 and lifted with trypsin. Trypsin was quenched with DMEM containing 10% FBS and cells were collected at 500
531 g for 5 min at RT. Cells were fixed in PBS containing 2% paraformaldehyde for 10 min at RT, then washed
532 and resuspended in PBS. Samples were analyzed using an AttuneNxT flow cytometer. Cells were identified
533 using FSC-A and SSC-A, and single cells were gated using FSC-W and FSC-H. BL-1 laser (488nm) was used
534 to identify GFP+ cells, and only cells with median GFP intensities 10-fold above background were considered
535 positive.

Virus particle binding. nHDF or ARPE19 cells were seeded at density of 35,000 cells per cm^2 on chamber slides (Nunc Lab Tek II). 2 days later, virus stocks were diluted with media to equal numbers of virus particles based on genome quantification by qPCR. Binding of virus particles to the cells was allowed for 20min at 37°C. Then the inoculum was removed, and the cells were washed once with medium to remove unbound virus before fixation and permeabilization with 80% acetone for 5min. Bound virus particles were stained with an antibody against the capsid-associated tegument protein pp150 (64) which allowed to detect enveloped particles attached to the plasma membrane as well as internalized particles. For visualization, a goat anti-mouse Alexa Fluor 488 (Invitrogen) secondary antibody was used. Unbound secondary antibody was washed off before the chambers were removed and the cells were mounted with medium containing DAPI (Fluoroshield) and sealed with a cover slide for later immunofluorescence analysis. Images were taken with a Leica DM5500 at 630-fold magnification. For each sample 10 images with 4 to 6 cells per image were taken and the number of cell nuclei as well as the number of virus particles was determined using Fuji software. Three independent virus stocks were tested in 3 independent experiments.

Antibody neutralization assays. Equal numbers of nHDF-derived cell-free parental viruses and heterologous gO recombinants were incubated with multiple concentrations of anti-gH mAb 14-4b or AP86 for 1hr at RT then plated on nHDF or ARPE19 for 4hrs at 37°C. Cells were then cultured in the appropriate growth medium supplemented with 2% FBS. After 2 days, cells were detected from the dish and fixed for flow cytometry analyses. Each antibody concentration was performed in triplicate and 3 independent experiments were conducted.

ACKNOWLEDGMENTS

We are grateful to Bill Britt, David Johnson, Jay Nelson, and Richard Stanton for generously supplying HCMV BAC clones, antibodies, and cell lines as indicated in the Material and Methods, and members of the Ryckman laboratory for support, and insightful discussions. We also thank Ekaterina Voronina and Mary Ellenbecker of University of Montana for assistance with immunofluorescent microscopy, the staff of the University of Montana Center for Biomolecular Structure and Dynamics Integrated Structural Biology Core Facility for help purifying monoclonal antibodies, and the staff of the University of Montana Flow Cytometry Core of the Center for Environmental Heath Sciences for assistance with flow cytometry.

This work was supported by grant from the National Institutes of Health to B.J.R (R01AI097274), a fellowship from the German Research Foundation (DFG) to C.S. (STE 2835/1-1), a fellowship from American Heart Association to E.P.S (17POST33350043) and a National Institutes of Health CoBRE award to Center for Biomolecular Structure and Dynamics at University of Montana (PG20GM103546).

Experiments were designed by B.J.R., L.Z.D, C.S., and E.P.S, and performed by L.Z. and C.S. Critical reagents were developed by L.Z.D., J.M.L. and Q.Y. Data were analyzed, and manuscript was prepared by B.J.R., L.Z.D., C.S., Q.Y., E.P.S., and J.M.L.

REFERENCES

1. Cudini, J., S. Roy, C. J. Houldcroft, J. M. Bryant, D. P. Depledge, H. Tutill, P. Veys, R. Williams, A. J. J. Worth, A. U. Tamuri, R. A. Goldstein, and J. Breuer. 2019. Human cytomegalovirus haplotype reconstruction reveals high diversity due to superinfection and evidence of within-host recombination. *Proceedings of the National Academy of Sciences* 116: 5693-5698.
2. Hage, E., G. S. Wilkie, S. Linnenweber-Held, A. Dhingra, N. M. Suárez, J. J. Schmidt, P. C. Kay-Fedorov, E. Mischak-Weissinger, A. Heim, A. Schwarz, T. F. Schulz, A. J. Davison, and T. Ganzenmueller. 2017. Characterization of Human Cytomegalovirus Genome Diversity in Immunocompromised Hosts by Whole-Genome Sequencing Directly From Clinical Specimens. *The Journal of Infectious Diseases* 215: 1673-1683.
3. Lassalle, F., D. P. Depledge, M. B. Reeves, A. C. Brown, M. T. Christiansen, H. J. Tutill, R. J. Williams, K. Einer-Jensen, J. Holdstock, C. Atkinson, J. R. Brown, F. B. van Loenen, D. A. Clark, P. D. Griffiths, G. M. G. M. Verjans, M. Schutten, R. S. B. Milne, F. Balloux, and J. Breuer. 2016. Islands of linkage in an ocean of pervasive recombination reveals two-speed evolution of human cytomegalovirus genomes. *Virus Evol* 2: vew017.
4. Renzette, N., B. Bhattacharjee, J. D. Jensen, L. Gibson, and T. F. Kowalik. 2011. Extensive genome-wide variability of human cytomegalovirus in congenitally infected infants. *PLoS Pathog* 7: e1001344.
5. Renzette, N., L. Gibson, B. Bhattacharjee, D. Fisher, M. R. Schleiss, J. D. Jensen, and T. F. Kowalik. 2013. Rapid Intrahost Evolution of Human Cytomegalovirus Is Shaped by Demography and Positive Selection. *PLoS Genet* 9: e1003735.
6. Sijmons, S., K. Thys, M. Mbong Ngwese, E. Van Damme, J. Dvorak, M. Van Loock, G. Li, R. Tachezy, L. Busson, J. Aerssens, M. Van Ranst, and P. Maes. 2015. High-throughput analysis of human cytomegalovirus genome diversity highlights the widespread occurrence of gene-disrupting mutations and pervasive recombination. *J Virol*
7. Suarez, N., K. G. Musonda, E. Escriva, M. Njenga, A. Agbueze, S. Camiolo, A. J. Davison, and U. A. Gompels. 2018. Multiple-Strain Infections of Human Cytomegalovirus with High Genomic Diversity are Common In Breast Milk from HIV-Positive Women in Zambia.
8. Suárez, N. M., G. S. Wilkie, E. Hage, S. Camiolo, M. Holton, J. Hughes, M. D. Maabar, V. B. Sreenu, A. Dhingra, U. A. Gompels, G. W. G. Wilkinson, F. Baldanti, M. Furione, D. Lilleri, A. Arossa, T. Ganzenmueller, G. Gerna, P. Hubáček, T. F. Schulz, D. Wolf, M. Zavattoni, and A. J. Davison. 2019. Human Cytomegalovirus Genomes Sequenced Directly from Clinical Material: Variation, Multiple-Strain Infection, Recombination and Gene Loss. *J Infect Dis*
9. Zhou, M., Q. Yu, A. Wechsler, and B. J. Ryckman. 2013. Comparative analysis of gO isoforms reveals that strains of human cytomegalovirus differ in the ratio of gH/gL/gO and gH/gL/UL128-131 in the virion envelope. *J Virol* 87: 9680-9690.
10. Rasmussen, L., A. Geissler, C. Cowan, A. Chase, and M. Winters. 2002. The genes encoding the gCIII complex of human cytomegalovirus exist in highly diverse combinations in clinical isolates. *J Virol* 76: 10841-10848.
11. Stanton, R., D. Westmoreland, J. D. Fox, A. J. Davison, and G. W. Wilkinson. 2005. Stability of human cytomegalovirus genotypes in persistently infected renal transplant recipients. *J Med Virol* 75: 42-46.
12. Mattick, C., D. Dewin, S. Polley, E. Sevilla-Reyes, S. Pignatelli, W. Rawlinson, G. Wilkinson, P. Dal Monte, and U. A. Gompels. 2004. Linkage of human cytomegalovirus glycoprotein gO variant groups identified from worldwide clinical isolates with gN genotypes, implications for disease associations and evidence for N-terminal sites of positive selection. *Virology* 318: 582-597.
13. Gorzer, I., C. Guelly, S. Trajanoski, and E. Puchhammer-Stockl. 2010. Deep sequencing reveals highly complex dynamics of human cytomegalovirus genotypes in transplant patients over time. *J Virol* 84: 7195-7203.
14. Cooper, R. S., and E. E. Heldwein. 2015. Herpesvirus gB: A Finely Tuned Fusion Machine. *Viruses* 7: 6552-6569.
15. Heldwein, E. E. 2016. gH/gL supercomplexes at early stages of herpesvirus entry. *Curr Opin Virol* 18: 1-

8.
16. Connolly, S. A., J. O. Jackson, T. S. Jardetzky, and R. Longnecker. 2011. Fusing structure and function: a structural view of the herpesvirus entry machinery. *Nat Rev Microbiol* 9: 369-381.
17. Wang, D., and T. Shenk. 2005. Human cytomegalovirus virion protein complex required for epithelial and endothelial cell tropism. *Proc Natl Acad Sci U S A* 102: 18153-18158.
18. Li, L., J. A. Nelson, and W. J. Britt. 1997. Glycoprotein H-related complexes of human cytomegalovirus: identification of a third protein in the gCIII complex. *J Virol* 71: 3090-3097.
19. Huber, M. T., and T. Compton. 1997. Characterization of a novel third member of the human cytomegalovirus glycoprotein H-glycoprotein L complex. *J Virol* 71: 5391-5398.
20. Vanarsdall, A. L., P. W. Howard, T. W. Wisner, and D. C. Johnson. 2016. Human Cytomegalovirus gH/gL Forms a Stable Complex with the Fusion Protein gB in Virions. *PLoS Pathog* 12: e1005564.
21. Hahn, G., M. G. Revello, M. Patrone, E. Percivalle, G. Campanini, A. Sarasini, M. Wagner, A. Gallina, G. Milanesi, U. Koszinowski, F. Baldanti, and G. Gerna. 2004. Human cytomegalovirus UL131-128 genes are indispensable for virus growth in endothelial cells and virus transfer to leukocytes. *J Virol* 78: 10023-10033.
22. Jiang, X. J., B. Adler, K. L. Sampaio, M. Digel, G. Jahn, N. Ettischer, Y. D. Stierhof, L. Scrivano, U. Koszinowski, M. Mach, and C. Sinzger. 2008. UL74 of human cytomegalovirus contributes to virus release by promoting secondary envelopment of virions. *J Virol* 82: 2802-2812.
23. Ryckman, B. J., M. A. Jarvis, D. D. Drummond, J. A. Nelson, and D. C. Johnson. 2006. Human cytomegalovirus entry into epithelial and endothelial cells depends on genes UL128 to UL150 and occurs by endocytosis and low-pH fusion. *J Virol* 80: 710-722.
24. Wang, D., and T. Shenk. 2005. Human cytomegalovirus UL131 open reading frame is required for epithelial cell tropism. *J Virol* 79: 10330-10338.
25. Wille, P. T., A. J. Knoche, J. A. Nelson, M. A. Jarvis, and D. C. Johnson. 2010. A human cytomegalovirus gO-null mutant fails to incorporate gH/gL into the virion envelope and is unable to enter fibroblasts and epithelial and endothelial cells. *J Virol* 84: 2585-2596.
26. Zhou, M., J. M. Lanchy, and B. J. Ryckman. 2015. Human cytomegalovirus gH/gL/gO promotes the fusion step of entry into all cell types whereas gH/gL/UL128-131 broadens virus tropism through a distinct mechanism. *J Virol*
27. Laib Sampaio, K., C. Stegmann, I. Brizic, B. Adler, R. J. Stanton, and C. Sinzger. 2016. The contribution of pUL74 to growth of human cytomegalovirus is masked in the presence of RL13 and UL128 expression. *J Gen Virol* 97: 1917-1927.
28. Wu, K., A. Oberstein, W. Wang, and T. Shenk. 2018. Role of PDGF receptor-α during human cytomegalovirus entry into fibroblasts. *Proc Natl Acad Sci U S A* 115: E9889-E9898.
29. E, X., P. Meraner, P. Lu, J. M. Perreira, A. M. Aker, W. M. McDougall, R. Zhuge, G. C. Chan, R. M. Gerstein, P. Caposio, A. D. Yurochko, A. L. Brass, and T. F. Kowalik. 2019. OR14I1 is a receptor for the human cytomegalovirus pentameric complex and defines viral epithelial cell tropism. *Proc Natl Acad Sci U S A* 116: 7043-7052.
30. Kabanova, A., J. Marcandalli, T. Zhou, S. Bianchi, U. Baxa, Y. Tsybovsky, D. Lilleri, C. Silacci-Fregni, M. Foglierini, B. M. Fernandez-Rodriguez, A. Druz, B. Zhang, R. Geiger, M. Pagani, F. Sallusto, P. D. Kwong, D. Corti, A. Lanzavecchia, and L. Perez. 2016. Platelet-derived growth factor-alpha receptor is the cellular receptor for human cytomegalovirus gHgLgO trimer. *Nat Microbiol* 2016:
31. Martinez-Martin, N., J. Marcandalli, C. S. Huang, C. P. Arthur, M. Perotti, M. Foglierini, H. Ho, A. M. Dosey, S. Shriver, J. Payandeh, A. Leitner, A. Lanzavecchia, L. Perez, and C. Ciferri. 2018. An Unbiased Screen for Human Cytomegalovirus Identifies Neuropilin-2 as a Central Viral Receptor. *Cell* 174: 1158-1171.e19.
32. Wu, Y., A. Prager, S. Boos, M. Resch, I. Brizic, M. Mach, S. Wildner, L. Scrivano, and B. Adler. 2017. Human cytomegalovirus glycoprotein complex gH/gL/gO uses PDGFR-α as a key for entry. *PLoS Pathog* 13: e1006281.
33. Stegmann, C., D. Hochdorfer, D. Lieber, N. Subramanian, D. Stöhr, K. Laib Sampaio, and C. Sinzger. 2017. A derivative of platelet-derived growth factor receptor alpha binds to the trimer of human cytomegalovirus and inhibits entry into fibroblasts and endothelial cells. *PLoS Pathog* 13: e1006273.

34. Vanarsdall, A. L., B. J. Ryckman, M. C. Chase, and D. C. Johnson. 2008. Human cytomegalovirus glycoproteins gB and gH/gL mediate epithelial cell-cell fusion when expressed either in cis or in trans. *J Virol* 82: 11837-11850.
35. Bogner, E., M. Reschke, B. Reis, E. Reis, W. Britt, and K. Radsak. 1992. Recognition of compartmentalized intracellular analogs of glycoprotein H of human cytomegalovirus. *Arch Virol* 126: 67-80.
36. Chiuppesi, F., F. Wussow, E. Johnson, C. Bian, M. Zhuo, A. Rajakumar, P. A. Barry, W. J. Britt, R. Chakraborty, and D. J. Diamond. 2015. Vaccine-Derived Neutralizing Antibodies to the Human Cytomegalovirus gH/gL Pentamer Potently Block Primary Cytotrophoblast Infection. *J Virol*
37. Fouts, A. E., P. Chan, J. P. Stephan, R. Vandlen, and B. Feierbach. 2012. Antibodies against the gH/gL/UL128/UL130/UL131 complex comprise the majority of the anti-cytomegalovirus (anti-CMV) neutralizing antibody response in CMV hyperimmune globulin. *J Virol* 86: 7444-7447.
38. Fouts, A. E., L. Comps-Agrar, K. F. Stengel, D. Ellerman, A. J. Schoeffler, S. Warming, D. L. Eaton, and B. Feierbach. 2014. Mechanism for neutralizing activity by the anti-CMV gH/gL monoclonal antibody MSL-109. *Proc Natl Acad Sci U S A* 111: 8209-8214.
39. Gerna, G., E. Percivalle, L. Perez, A. Lanzavecchia, and D. Lilleri. 2016. Monoclonal Antibodies to Different Components of the Human Cytomegalovirus (HCMV) Pentamer gH/gL/pUL128L and Trimer gH/gL/gO as well as Antibodies Elicited during Primary HCMV Infection Prevent Epithelial Cell Syncytium Formation. *J Virol* 90: 6216-6223.
40. Kabanova, A., L. Perez, D. Lilleri, J. Marcandalli, G. Agatic, S. Becattini, S. Preite, D. Fuschillo, E. Percivalle, F. Sallusto, G. Gerna, D. Corti, and A. Lanzavecchia. 2014. Antibody-driven design of a human cytomegalovirus gHgLpUL128L subunit vaccine that selectively elicits potent neutralizing antibodies. *Proc Natl Acad Sci U S A* 111: 17965-17970.
41. Nokta, M., M. D. Tolpin, P. I. Nadler, and R. B. Pollard. 1994. Human monoclonal anti-cytomegalovirus (CMV) antibody (MSL 109): enhancement of in vitro foscarnet- and ganciclovir-induced inhibition of CMV replication. *Antiviral Res* 24: 17-26.
42. Vanarsdall, A. L., A. L. Chin, J. Liu, T. S. Jardetzky, J. O. Mudd, S. L. Orloff, D. Streblow, M. M. Mussi-Pinhata, A. Y. Yamamoto, G. Duarte, W. J. Britt, and D. C. Johnson. 2019. HCMV trimer- and pentamer-specific antibodies synergize for virus neutralization but do not correlate with congenital transmission. *Proc Natl Acad Sci U S A* 116: 3728-3733.
43. Wussow, F., F. Chiuppesi, J. Martinez, J. Campo, E. Johnson, C. Flechsig, M. Newell, E. Tran, J. Ortiz, C. La Rosa, A. Herrmann, J. Longmate, R. Chakraborty, P. A. Barry, and D. J. Diamond. 2014. Human cytomegalovirus vaccine based on the envelope gH/gL pentamer complex. *PLoS Pathog* 10: e1004524.
44. Wei, X., J. M. Decker, S. Wang, H. Hui, J. C. Kappes, X. Wu, J. F. Salazar-Gonzalez, M. G. Salazar, J. M. Kilby, M. S. Saag, N. L. Komarova, M. A. Nowak, B. H. Hahn, P. D. Kwong, and G. M. Shaw. 2003. Antibody neutralization and escape by HIV-1. *Nature* 422: 307-312.
45. Kropff, B., C. Burkhardt, J. Schott, J. Nentwich, T. Fisch, W. Britt, and M. Mach. 2012. Glycoprotein N of human cytomegalovirus protects the virus from neutralizing antibodies. *PLoS Pathog* 8: e1002999.
46. Jiang, X. J., K. L. Sampaio, N. Ettischer, Y. D. Stierhof, G. Jahn, B. Kropff, M. Mach, and C. Sinzger. 2011. UL74 of human cytomegalovirus reduces the inhibitory effect of gH-specific and gB-specific antibodies. *Arch Virol*
47. Cui, X., D. C. Freed, D. Wang, P. Qiu, F. Li, T. M. Fu, L. M. Kauvar, and M. A. McVoy. 2017. Impact of Antibodies and Strain Polymorphisms on Cytomegalovirus Entry and Spread in Fibroblasts and Epithelial Cells. *J Virol* 91:
48. Zhang, L., M. Zhou, R. Stanton, J. Kamil, and B. J. Ryckman. 2018. Expression levels of glycoprotein O (gO) vary between strains of human cytomegalovirus, influencing the assembly of gH/gL complexes and virion infectivity. *J Virol*
49. Kalser, J., B. Adler, M. Mach, B. Kropff, E. Puchhammer-Stöckl, and I. Görzer. 2017. Differences in Growth Properties among Two Human Cytomegalovirus Glycoprotein O Genotypes. *Front Microbiol* 8: 1609.
50. Murrell, I., C. Bedford, K. Ladell, K. L. Miners, D. A. Price, P. Tomasec, G. W. G. Wilkinson, and R. J. Stanton. 2017. The pentameric complex drives immunologically covert cell-cell transmission of wild-type

human cytomegalovirus. *Proc Natl Acad Sci U S A*

51. Stanton, R. J., K. Baluchova, D. J. Dargan, C. Cunningham, O. Sheehy, S. Seirafian, B. P. McSharry, M. L. Neale, J. A. Davies, P. Tomasec, A. J. Davison, and G. W. Wilkinson. 2010. Reconstruction of the complete human cytomegalovirus genome in a BAC reveals RL13 to be a potent inhibitor of replication. *J Clin Invest* 120: 3191-3208.
52. Murrell, I., G. S. Wilkie, A. J. Davison, E. Statkute, C. A. Fielding, P. Tomasec, G. W. Wilkinson, and R. J. Stanton. 2016. Genetic Stability of Bacterial Artificial Chromosome-Derived Human Cytomegalovirus during Culture In Vitro. *J Virol* 90: 3929-3943.
53. Vanarsdall, A. L., T. W. Wisner, H. Lei, A. Kazlauskas, and D. C. Johnson. 2012. PDGF receptor-alpha does not promote HCMV entry into epithelial and endothelial cells but increased quantities stimulate entry by an abnormal pathway. *PLoS Pathog* 8: e1002905.
54. Liu, J., T. S. Jardetzky, A. L. Chin, D. C. Johnson, and A. L. Vanarsdall. 2018. The human cytomegalovirus trimer and pentamer promote sequential steps in entry into epithelial and endothelial cells at cell surfaces and endosomes. *Journal of Virology* JVI.01336-18.
55. Murrell, I., P. Tomasec, G. S. Wilkie, D. J. Dargan, A. J. Davison, and R. J. Stanton. 2013. Impact of sequence variation in the UL128 locus on production of human cytomegalovirus in fibroblast and epithelial cells. *J Virol* 87: 10489-10500.
56. Schultz, E. P., J. M. Lanchy, E. E. Ellerbeck, and B. J. Ryckman. 2015. Scanning Mutagenesis of Human Cytomegalovirus Glycoprotein gH/gL. *J Virol* 90: 2294-2305.
57. Urban, M., W. Britt, and M. Mach. 1992. The dominant linear neutralizing antibody-binding site of glycoprotein gp86 of human cytomegalovirus is strain specific. *J Virol* 66: 1303-1311.
58. Ourahmane, A., X. Cui, L. He, M. Catron, D. P. Dittmer, A. Al Qaffasaa, M. R. Schleiss, L. Hertel, and M. A. McVoy. 2019. Inclusion of Antibodies to Cell Culture Media Preserves the Integrity of Genes Encoding RL13 and the Pentameric Complex Components During Fibroblast Passage of Human Cytomegalovirus. *Viruses* 11:
59. Scrivano, L., C. Sinzger, H. Nitschko, U. H. Koszinowski, and B. Adler. 2011. HCMV spread and cell tropism are determined by distinct virus populations. *PLoS Pathog* 7: e1001256.
60. Stegmann, C., F. Rothemund, K. Laib Sampaio, B. Adler, and C. Sinzger. 2019. The N Terminus of Human Cytomegalovirus Glycoprotein O Is Important for Binding to the Cellular Receptor PDGFRα. *Journal of Virology* 93:
61. Murphy, E., D. Yu, J. Grimwood, J. Schmutz, M. Dickson, M. A. Jarvis, G. Hahn, J. A. Nelson, R. M. Myers, and T. E. Shenk. 2003. Coding potential of laboratory and clinical strains of human cytomegalovirus. *Proc Natl Acad Sci U S A* 100: 14976-14981.
62. Tischer, B. K., J. von Einem, B. Kaufer, and N. Osterrieder. 2006. Two-step red-mediated recombination for versatile high-efficiency markerless DNA manipulation in Escherichia coli. *Biotechniques* 40: 191-197.
63. Tischer, B. K., G. A. Smith, and N. Osterrieder. 2010. En passant mutagenesis: a two step markerless red recombination system. *Methods Mol Biol* 634: 421-430.
64. Sanchez, V., K. D. Greis, E. Sztul, and W. J. Britt. 2000. Accumulation of virion tegument and envelope proteins in a stable cytoplasmic compartment during human cytomegalovirus replication: characterization of a potential site of virus assembly. *J Virol* 74: 975-986.
65. Chee, M., S. A. Rudolph, B. Plachter, B. Barrell, and G. Jahn. 1989. Identification of the major capsid protein gene of human cytomegalovirus. *J Virol* 63: 1345-1353.

FIGURE LEGENDS

Figure 1. Immunoblot analysis of gH/gL complexes in parental and heterologous gO recombinant HCMV. Equal numbers of cell-free HCMV TR (A), ME (B), or MT (C) or the corresponding heterologous gO recombinants were separated by reducing (upper two panels) or non-reducing (bottom panel) SDS-PAGE, and analyzed by immunoblot with antibodies specific for major capsid protein (MCP) or gL. Blots shown are representative of three independent experiments. Molecular mass markers (kDa) indicated on each panel.

Figure 2. Relative fibroblast and epithelial cell tropism of parental and heterologous gO recombinant HCMV. Equal amounts of cell-free stocks of HCMV TR (A), ME (B), or MT (C) or the corresponding heterologous gO recombinants were plated on nHDF fibroblasts or ARPE-19 epithelial cells and the number of infected cells were determined at 2 days post infection. Ratios greater than or equal to 1 of the number of each cell type infected (fib/epi or epi/fib) are plotted for each of three independent sets of virus stocks (black, open and striped bars).

Figure 3. Specific infectivity of parental and heterologous gO recombinant HCMV. Extracellular HCMV stocks of HCMV TR (A), ME (B), or MT (C) or the corresponding heterologous gO recombinants were quantified by qPCR for viral genomes, and infectious units (IU) were determined by flow cytometry quantification of GFP-expressing nHDF fibroblasts or ARPE-19 epithelial cells, 2 days post infection. Average genomes/IU of 3 independent set of virus stock are plotted, with error bars representing standard deviations. P-values were generated by unpaired, two-tailed t-tests comparing each heterologous gO recombinant to the corresponding parental virus (*<0.05).

Figure 4. Binding of parental and heterologous gO recombinant HCMV to fibroblasts. Extracellular virions of HCMV TR, ME, MT or the corresponding heterologous gO recombinants were applied to nHDF for 20 min. After washing away unbound virus, cell-associated virus particles were detected by immunofluorescence using antibodies specific for the capsid-associated tegument protein pp150. Cells were visualized by staining nuclei with DAPI. Representative fields of parental TR, ME, MT and heterologous gO recombinants that consistently reduced binding in 3 independent experiments.

.

Figure 5. Spread of parental and heterologous gO recombinant HCMV in fibroblast cultures. Confluent monolayers of nHDF or HFFFTet (for “MT”) were infected at MOI 0.003 with HCMV TR (A, B), ME (A, C), MT (A, D) or the corresponding heterologous gO recombinants. At 3 and 12 days post infection cultures were analyzed by fluorescence microscopy (A) or by flow cytometry to quantitate the total number of infected (GFP+) cells (B-D). Plotted are the average number of infected cells at day 12 per infected cell at day 3 in 3 independent experiments. Error bars represent standard deviations. P-values were generated by unpaired, two-tailed t-test comparing each heterologous gO recombinant to the corresponding parental virus (*<0.05).

Figure 6. Release of extracellular progeny by parental and heterologous gO recombinant HCMV in fibroblast cultures. Cultures of nHDF or HFFFTet (for “MT”) were infected at MOI 1 with HCMV TR (A), ME (B), MT (C) or the corresponding heterologous gO recombinants for 8 days. The number of infected cells was determined by flow cytometry and progeny virus in culture supernatants was quantified by qPCR for viral genomes. The average number of extracellular virions per infected cell in each of 3 independent experiments is plotted. Error bars represent standard deviations and P-values were generated by unpaired two-tailed t-test comparing each heterologous gO recombinant to the corresponding parental virus (*<0.05).

Figure 7. Spread of parental and heterologous gO recombinant HCMV in epithelial cell cultures. Confluent monolayers of ARPE19 cells were infected at MOI 0.003 of HCMV TR (A, B), ME (A, C), or the corresponding heterologous gO recombinants. At 3 and 12 days post infection cultures were analyzed by fluorescence microscopy (A) or by flow cytometry to quantitate the total number of infected (GFP+) cells (B-D). Plotted are the average number of infected cells at day 12 per infected cell at day 3 in 3 independent experiments. Error bars represent standard deviations. P-values were generated by unpaired, two-tailed t-test comparing each heterologous gO recombinant to the corresponding parental virus (*<0.05)

.

Figure 8. Neutralization of parental HCMV TR and heterologous gO recombinant by anti-gH antibodies. Equal numbers of extracellular HCMV TR or the corresponding heterologous gO recombinants were incubated with 0.025-250 μg/mL of anti-gH mAb 14-4b, or 0.01-100 μg/mL of anti-gH mAb AP86 and then plated on cultures of nHDF fibroblasts (A and B) or ARPE19 epithelial cells (C and D). At 2 days post infection the number of infected (GFP+) cells was determined by flow cytometry and plotted as the percent of the no antibody control. (Left panels) Full titration curves shown are representative of three independent experiments, each performed in triplicate. (Right panels) Average percent of cells infected at the highest antibody concentrations in 3 independent experiments. Error bars represent standard deviations. P-values were generated by unpaired, two-tailed t-test comparing each heterologous gO recombinant to the corresponding parental virus (*<0.05).

Figure 9. Neutralization of parental HCMV MT and heterologous gO recombinant by anti-gH antibodies. Equal numbers of extracellular HCMV MT or the corresponding heterologous gO recombinants were incubated with 0.025-250 μg/mL of anti-gH mAb 14-4b and then plated on cultures of nHDF fibroblasts (A) or ARPE19 epithelial cells (B). At 2 days post infection the number of infected (GFP+) cells was determined by flow cytometry and plotted as the percent of the no antibody control. (Left panels) Full titration curves shown are representative of three independent experiments, each performed in triplicate. (Right panels) Average percent of cells infected at the highest antibody concentrations in 3 independent experiments. Error bars represent standard deviations. P-values were generated by unpaired, two-tailed t-test comparing each heterologous gO recombinant to the corresponding parental virus (*<0.05).

Table 1. Immunoblot band density analyses of parental and heterologous gO recombinants

Genotype Background	Virion Protein(s) Analyzed							
TR	MCP		gL		gH/gL/gO		gH/gL/UL128	
gO genotype	Fold[b]	p-value[c]	Fold	p-value	Fold	p-value	Fold	p-value
TR(GT1b)	-	-	-	-	-	-	-	-
MEgO(GT5)	1.1	0.20	0.6	0.10	1.4	0.04	2.0	0.06
PHgO(GT2a)	1.1	0.40	0.9	0.30	1.8	0.02	2.3	0.01
TBgO (GT1c)	1.2	0.30	0.8	0.04	0.9	0.50	0.9	0.80
ADgO (GT1a)	1.1	0.60	0.9	0.09	0.9	0.30	1.0	0.70
TNgO (GT4)	1.1	0.50	2.0	0.10	2.7	0.10	2.1	0.30
ME	MCP		gL		gH/gL/gO		gH/gL/UL128	
gO genotype	Fold[b]	p-value[c]	Fold	p-value	Fold	p-value	Fold	p-value
MEgO(GT5)	-	-	-	-	-	-	-	-
TR(GT1b)	0.9	0.30	0.8	0.30	0.9	0.60	1.1	0.70
PHgO(GT2a)	1.1	0.30	1.1	0.70	1.4	0.40	1.4	0.40
TBgO (GT1c)	1.3	0.20	1.2	0.20	1.0	1.00	1.4	0.30
ADgO (GT1a)	1.0	0.70	0.7	0.30	0.9	0.50	1.1	0.70
TNgO (GT4)	1.1	0.30	0.8	0.40	0.9	0.70	1.4	0.10
MT	MCP		gL		gH/gL/gO		gH/gL/UL128	
gO genotype	Fold[b]	p-value[c]	Fold	p-value	Fold	p-value	Fold	p-value
MEgO(GT5)	-	-	-	-	-	-	-	-
TR(GT1b)	1.1	0.40	1.2	0.30	0.7	0.20	0.9	0.60
PHgO(GT2a)	1.1	0.40	1.6	0.20	1.4	0.40	1.1	0.80
TBgO (GT1c)	1.1	0.50	1.3	0.10	1.1	0.80	1.6	0.20
ADgO (GT1a)	0.8	0.30	0.5	0.40	0.6	0.30	1.7	0.04
TNgO (GT4)	0.9	0.10	0.7	0.40	1.4	0.10	1.8	0.20

a. Three independent stocks of cell-free virions collected from infected nHDF (for TR and ME) or HFFF-tet (for MT) culture supernatants and analyzed by immunoblot as described for Figure 1.
b. Mean fold difference of chemiluminescent band densities obtained for each recombinant compared to the parental TR in three independent experiments.
c. Two-tailed, paired t-test comparing each recombinant to the parental Merlin-T in three independent experiments.

Table 2. Binding of parental and heterologous gO recombinant HCMV to fibroblasts.

Genotype Background	Experiment 1 (input[a])			Experiment 2 (input)			Experiment 3 (input)		
TR	(6.2×10^7)			(7.5×10^7)			(1.0×10^8)		
gO genotype	Mean[b]	Fold[c]	p-value[d]	Mean	Fold	p-value	Mean	Fold	p-value
TR(GT1b)	17.8	-	-	31.2	-	-	30.4	-	-
MEgO(GT5)	21.2	-	0.8	44.7	-	0.0009	37.9	-	0.1
PHgO(GT2a)	24.3	-	0.4	12.7	-	0.0001	35.3	-	0.3
TBgO (GT1c)	18.8	-	0.6	30.5	-	0.8	33.7	-	0.4
ADgO (GT1a)	25.7	-	0.7	24.7	-	0.01	23.3	-	0.1
TNgO (GT4)[e]	**4.9**	**>3.6**	**0.007**	**6.9**	**>4.5**	**0.0001**	**7.3**	**>4.2**	**0.0001**
ME	(2.0×10^8)			(5.0×10^8)			(5.0×10^8)		
gO genotype	Mean	Fold	p-value	Mean	Fold	p-value	Mean	Fold	p-value
MEgO(GT5)	21.6	-	-	5.8	-	-	7	-	-
TR(GT1b)	5.3	-	0.0001	7.1	-	0.3	3.9	-	0.0002
PHgO(GT2a)	8.0	-	0.0001	7.5	-	0.09	2.3	-	0.0001
TBgO (GT1c)	15.9	-	0.02	9.0	-	0.07	7	-	1.0
ADgO (GT1a)	**2.4**	**>9**	**0.0001**	**2.4**	**>2.4**	**0.0001**	**3.7**	**>1.9**	**0.0001**
TNgO (GT4)	5.8	-	0.0001	8.5	-	0.03	7.4	-	0.7
MT	(1.0×10^8)			(2.0×10^8)			(5.0×10^8)		
gO genotype	Mean	Fold	p-value	Mean	Fold	p-value	Mean	Fold	p-value
MEgO(GT5)	27.5	-	-	63.9	-	-	120.9	-	-
TR(GT1b)	28.5	-	0.7	40.2	-	0.003	159.4	-	0.09
PHgO(GT2a)	33.4	-	0.09	50.4	-	0.06	222	-	0.0002
TBgO (GT1c)	44.6	-	0.0001	66.2	-	0.8	220.8	-	0.0005
ADgO (GT1a)	**8.5**	**>3.2**	**0.0001**	**13.4**	**>4.7**	**0.0001**	**23.6**	**>5.1**	**0.0001**
TNgO (GT4)	32.5	-	0.1	61.8	-	0.8	133.2	-	0.3

a. Concentration of cell-free virus stock (genomes/mL) applied to cells.
b. Average pp150 puncta detected by immunofluorescence per cell in 10 microscopy fields; approximately 4 to 6 cells per field.
c. Fold difference in mean pp150 puncta per cell as compared to parental virus. Determined for recombinant viruses that were significantly different ($p \leq 0.05$) from parental in all three experiments. Indicated as fold greater than (<) or less than (>) parental. (-) indicates value not calculated.
d. P-values as determined by 2-tailed, unpaired T-test comparing each recombinant virus to the parental.
e. Bold font indicates recombinant viruses that were significantly different from the parental in the same direction (> or <) in all 3 experiments.

Table 3. Binding of parental and heterologous gO recombinant HCMV to epithelial cells.

Genotype Background	Experiment 1 (input[a])			Experiment 2 (input)			Experiment 3 (input)		
TR	(6.2×10^7)			(7.5×10^7)			(1.0×10^8)		
gO genotype	Mean[b]	Fold[c]	p-value[d]	Mean	Fold	p-value	Mean	Fold	p-value
TR(GT1b)	26.2	-	-	41.7	-	-	43.7	-	-
MEgO(GT5)	35.5	-	0.008	38.3	-	0.5	56.8	-	0.0001
PHgO(GT2a)	33.4	<1.3	0.008	19.3	>2.2	0.0001	61	<1.4	0.01
TBgO (GT1c)	24.1	-	0.2	35.4	-	0.2	58.7	-	0.02
ADgO (GT1a)	36.4	<1.4	0.003	22.2	>1.9	0.0002	36	>1.2	0.03
TNgO (GT4)[e]	**16.2**	**>1.6**	**0.0006**	**18.62**	**>2.2**	**0.0001**	**23.4**	**>1.9**	**0.0001**
ME	(2.0×10^8)			(5.0×10^8)			(5.0×10^8)		
gO genotype	Mean	Fold	p-value	Mean	Fold	p-value	Mean	Fold	p-value
MEgO(GT5)	37.3	-	-	18	-	-	15	-	-
TR(GT1b)	17.7	>2.1	0.0001	24.9	<1.4	0.03	10.4	>1.4	0.006
PHgO(GT2a)	22.3	>1.6	0.0001	23	<1.2	0.02	9.4	>1.6	0.002
TBgO (GT1c)	34.1	-	0.2	32.3	-	0.0001	18.6	-	0.09
ADgO (GT1a)	**14.4**	**>2.6**	**0.0001**	**11.4**	**>1.6**	**0.01**	**10.8**	**>1.4**	**0.01**
TNgO (GT4)	24.4	-	0.0001	25.9	-	0.01	14.3	-	0.6
MT	(1.0×10^8)			(2.0×10^8)			(5.0×10^8)		
gO genotype	Mean	Fold	p-value	Mean	Fold	p-value	Mean	Fold	p-value
MEgO(GT5)	33.2	-	-	68	-	-	236.8	-	-
TR(GT1b)	35.3	-	0.7	46.1	-	0.003	210.1	-	0.2
PHgO(GT2a)	46.5	-	0.009	78	-	0.2	383.2	-	0.0002
TBgO (GT1c)	63.4	-	0.0005	69.6	-	0.8	238.3	-	1.0
ADgO (GT1a)	**16.7**	**>2.0**	**0.0003**	**26.1**	**>2.6**	**0.0001**	**26.6**	**>8.9**	**0.0001**
TNgO (GT4)	44.1	<1.3	0.09	48.1	>1.4	0.009	150.9	>1.6	0.0003

a. Concentration of cell-free virus stock (genomes/mL) applied to cells.
b. Average pp150 puncta detected by immunofluorescence per cell in 10 microscopy fields; approximately 4 to 6 cells per field.
c. Fold difference in mean pp150 puncta per cell as compared to parental virus. Determined for recombinant viruses that were significantly different ($p \leq 0.05$) from parental in all three experiments. Indicated as fold greater than (<) or less than (>) parental. (-) indicates value not calculated.
d. P-values as determined by 2-tailed, unpaired T-test comparing each recombinant virus to the parental.
e. Bold font indicates recombinant viruses that were significantly different from the parental in the same direction (> or <) in all 3 experiments.

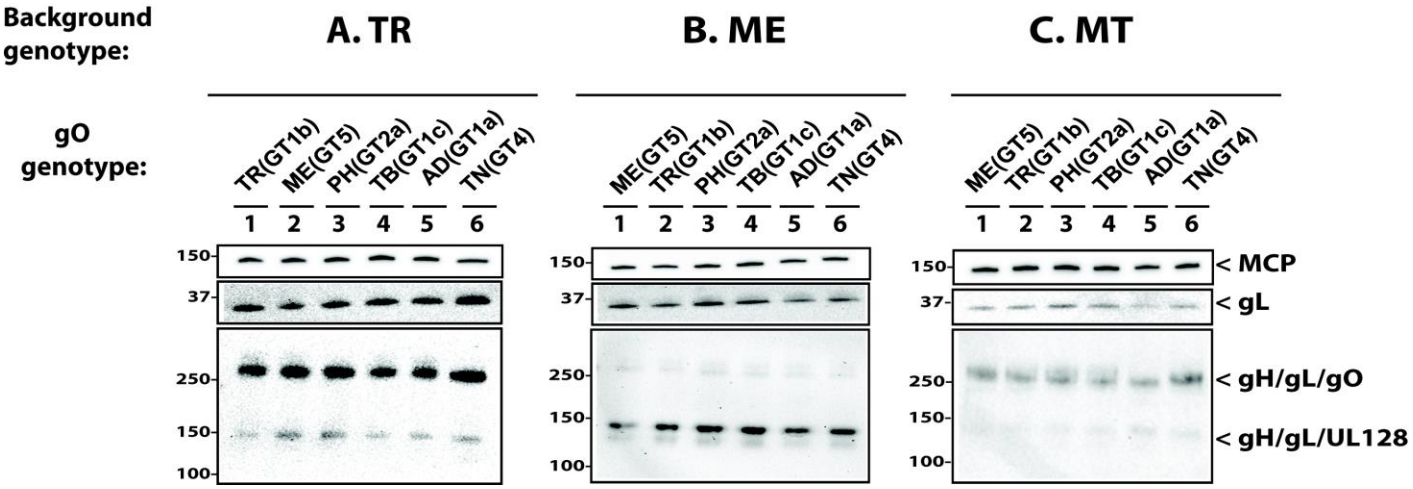

Figure 1. Immunoblot analysis of gH/gL complexes in parental and heterologous gO recombinant HCMV. Equal numbers of cell-free HCMV TR (A), ME (B), or MT (C) or the corresponding heterologous gO recombinants were separated by reducing (upper two panels) or non-reducing (bottom panel) SDS-PAGE, and analyzed by immunoblot with antibodies specific for major capsid protein (MCP) or gL. Blots shown are representative of three independent experiments. Molecular mass markers (kDa) indicated on each panel.

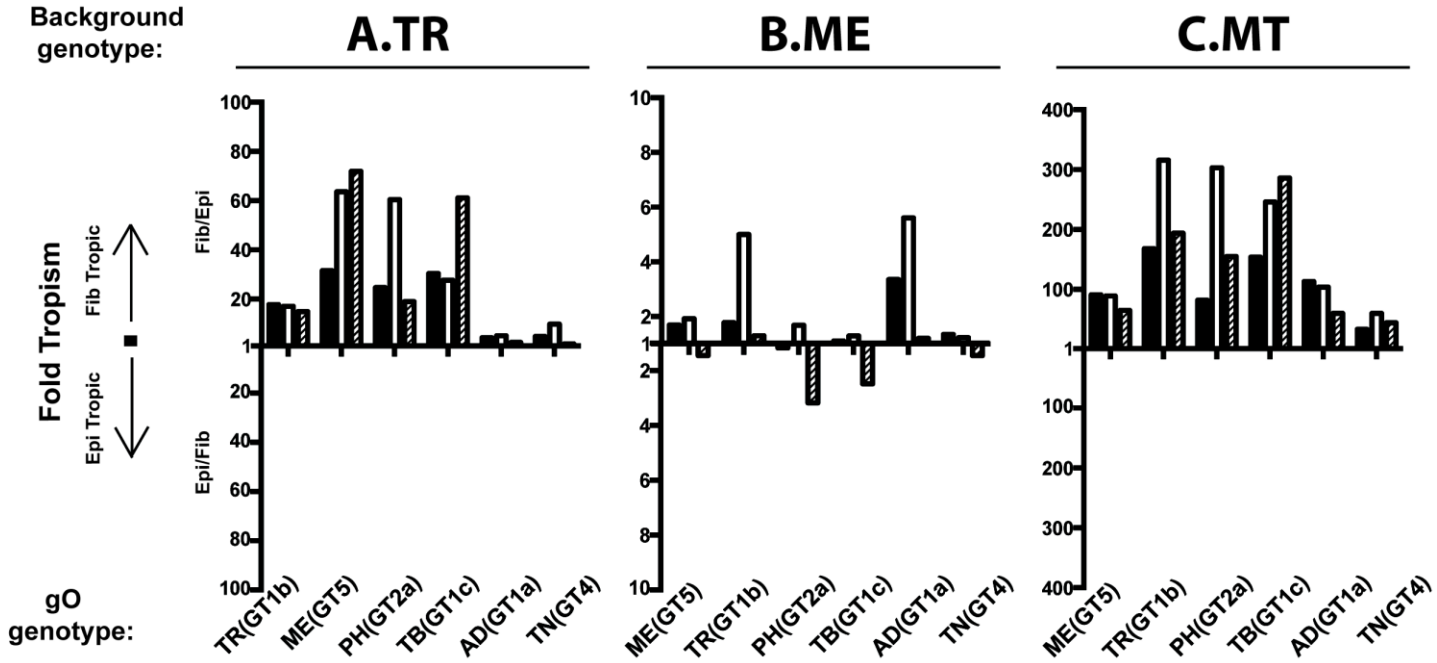

Figure 2. Relative fibroblast and epithelial cell tropism of parental and heterologous gO recombinant HCMV. Equal amounts of cell-free stocks of HCMV TR (A), ME (B), or MT (C) or the corresponding heterologous gO recombinants were plated on nHDF fibroblasts or ARPE-19 epithelial cells and the number of infected cells were determined at 2 days post infection. Ratios greater than or equal to 1 of the number of each cell type infected (fib/epi or epi/fib) are plotted for each of three independent sets of virus stocks (black, open and striped bars).

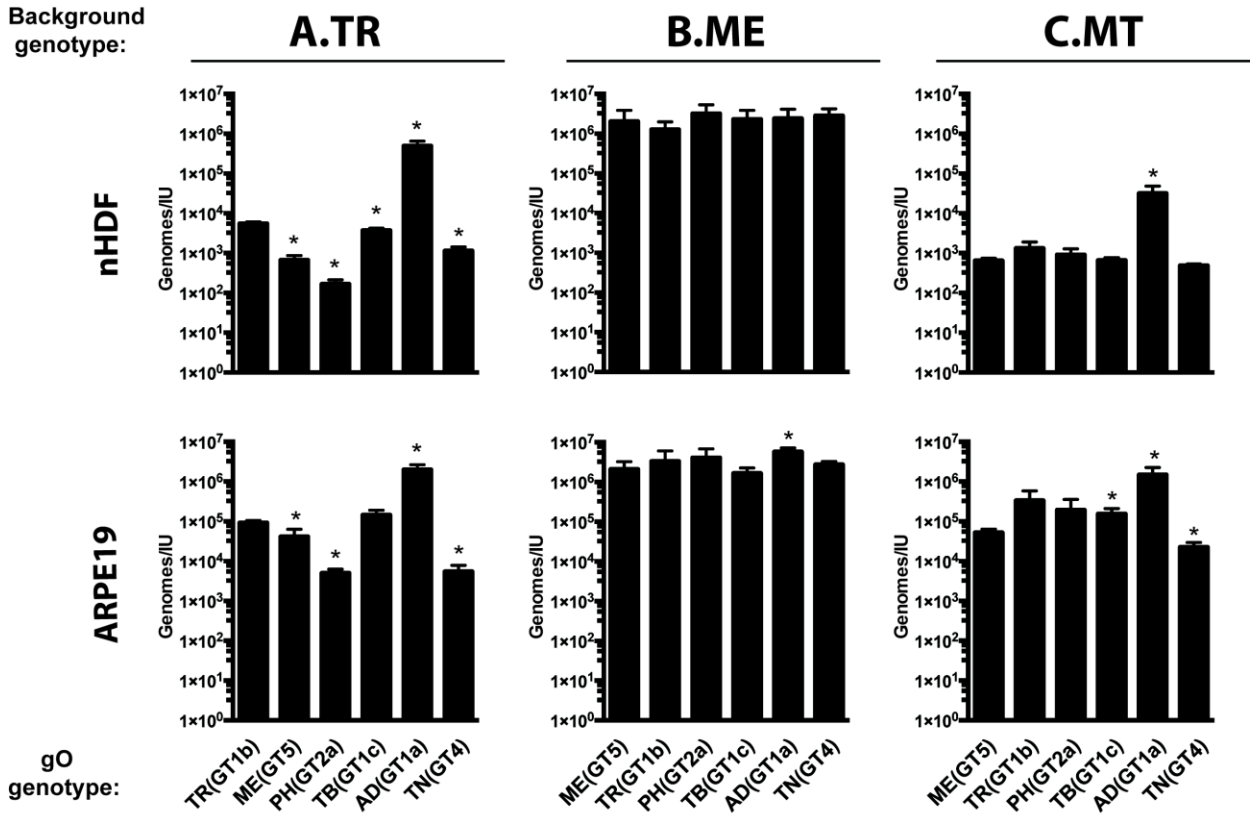

Figure 3. Specific infectivity of parental and heterologous gO recombinant HCMV. Extracellular HCMV stocks of HCMV TR (A), ME (B), or MT (C) or the corresponding heterologous gO recombinants were quantified by qPCR for viral genomes, and infectious units (IU) were determined by flow cytometry quantification of GFP-expressing nHDF fibroblasts or ARPE-19 epithelial cells, 2 days post infection. Average genomes/IU of 3 independent set of virus stock are plotted, with error bars representing standard deviations. P-values were generated by unpaired, two-tailed t-tests comparing each heterologous gO recombinant to the corresponding parental virus (*<0.05).

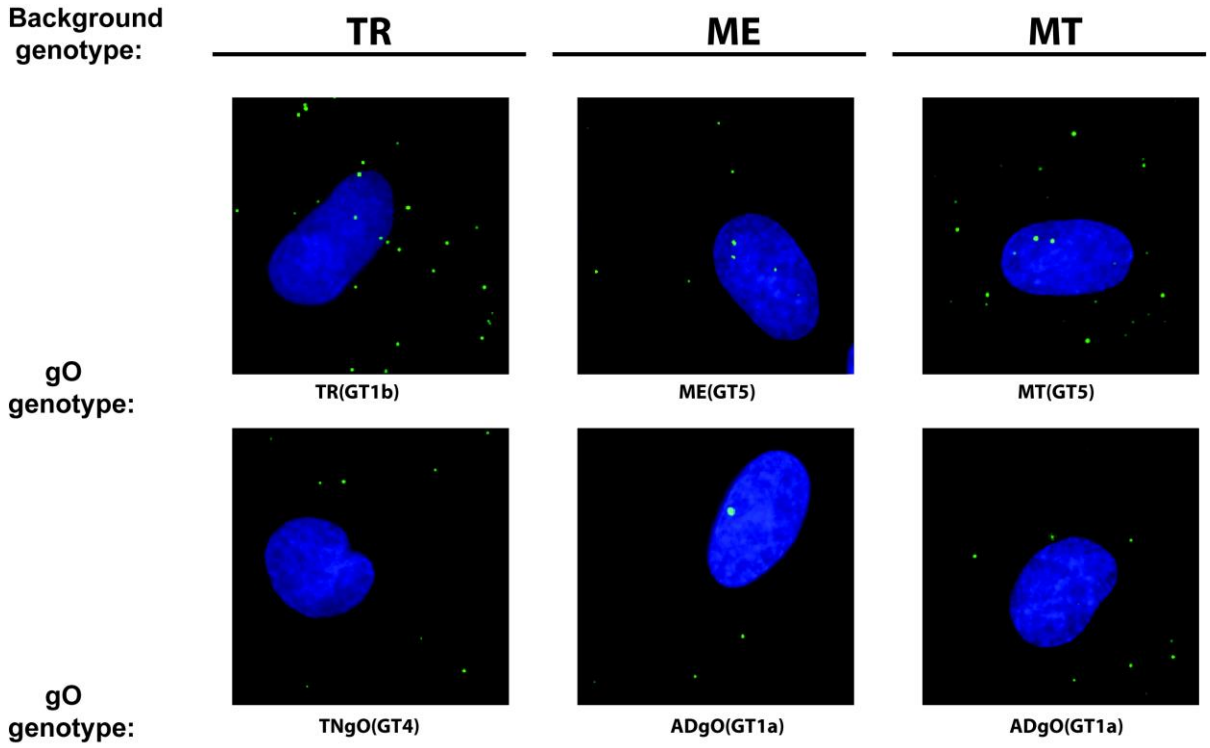

Figure 4. Binding of parental and heterologous gO recombinant HCMV to fibroblasts. Extracellular virions of HCMV TR, ME, MT or the corresponding heterologous gO recombinants were applied to nHDF for 20 min. After washing away unbound virus, cell-associated virus particles were detected by immunofluorescence using antibodies specific for the capsid-associated tegument protein pp150. Cells were visualized by staining nuclei with DAPI. Representative fields of parental TR, ME, MT and heterologous gO recombinants that consistently reduced binding in 3 independent experiments.

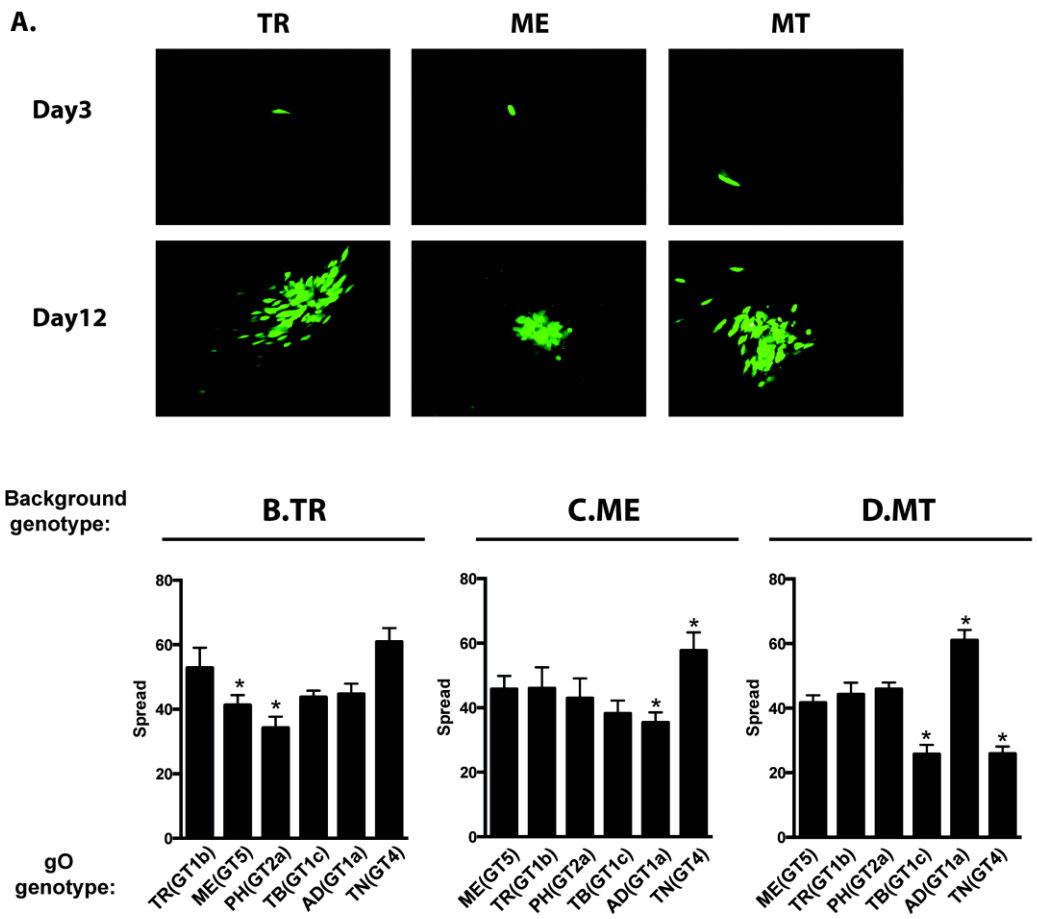

Figure 5. Spread of parental and heterologous gO recombinant HCMV in fibroblast cultures. Confluent monolayers of nHDF or HFFFTet (for "MT") were infected at MOI 0.003 with HCMV TR (A, B), ME (A, C), MT (A, D) or the corresponding heterologous gO recombinants. At 3 and 12 days post infection cultures were analyzed by fluorescence microscopy (A) or by flow cytometry to quantitate the total number of infected (GFP+) cells (B-D). Plotted are the average number of infected cells at day 12 per infected cell at day 3 in 3 independent experiments. Error bars represent standard deviations. P-values were generated by unpaired, two-tailed t-test comparing each heterologous gO recombinant to the corresponding parental virus (*<0.05).

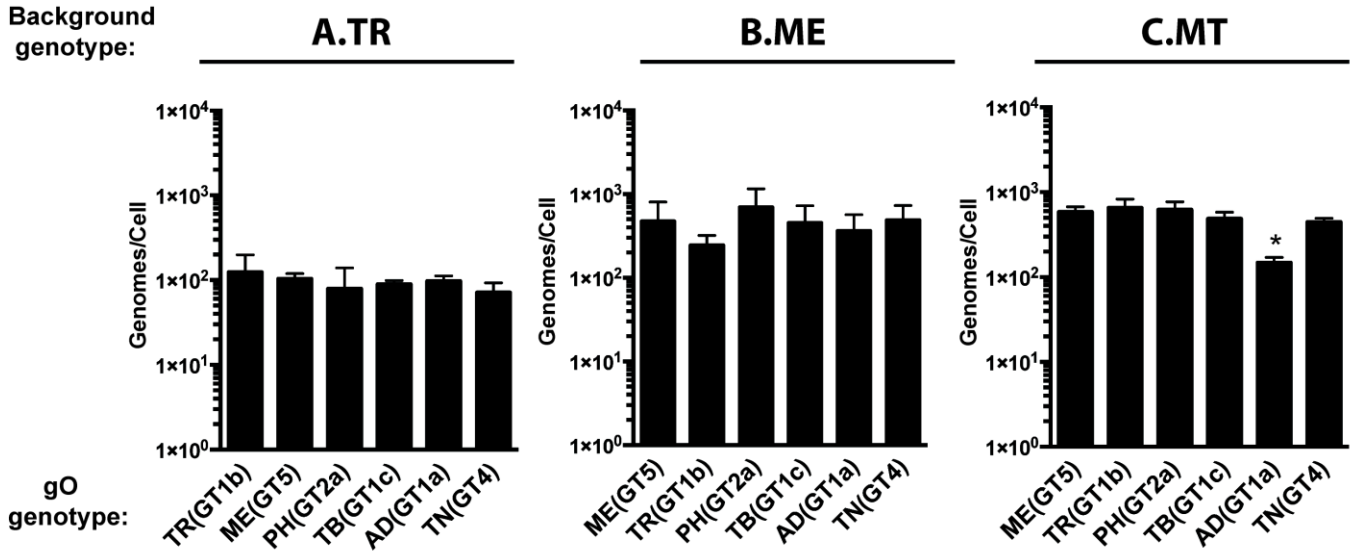

Figure 6. Release of extracellular progeny by parental and heterologous gO recombinant HCMV in fibroblast cultures. Cultures of nHDF or HFFFTet (for "MT") were infected at MOI 1 with HCMV TR (A), ME (B), MT (C) or the corresponding heterologous gO recombinants for 8 days. The number of infected cells was determined by flow cytometry and progeny virus in culture supernatants was quantified by qPCR for viral genomes. The average number of extracellular virions per infected cell in each of 3 independent experiments is plotted. Error bars represent standard deviations and P-values were generated by unpaired two-tailed t-test comparing each heterologous gO recombinant to the corresponding parental virus (*<0.05).

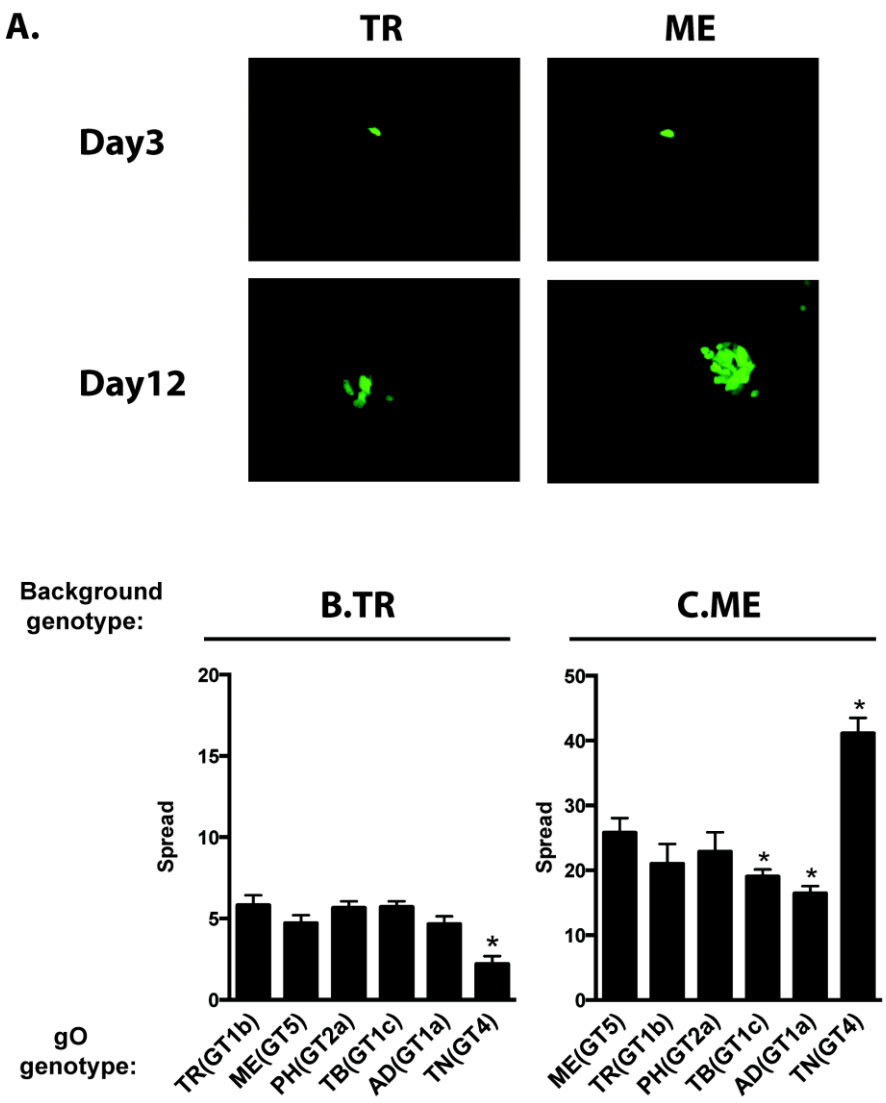

Figure 7. Spread of parental and heterologous gO recombinant HCMV in epithelial cell cultures. Confluent monolayers of ARPE19 cells were infected at MOI 0.003 of HCMV TR (A, B), ME (A, C), or the corresponding heterologous gO recombinants. At 3 and 12 days post infection cultures were analyzed by fluorescence microscopy (A) or by flow cytometry to quantitate the total number of infected (GFP+) cells (B-D). Plotted are the average number of infected cells at day 12 per infected cell at day 3 in 3 independent experiments. Error bars represent standard deviations. P-values were generated by unpaired, two-tailed t-test comparing each heterologous gO recombinant to the corresponding parental virus (*<0.05).

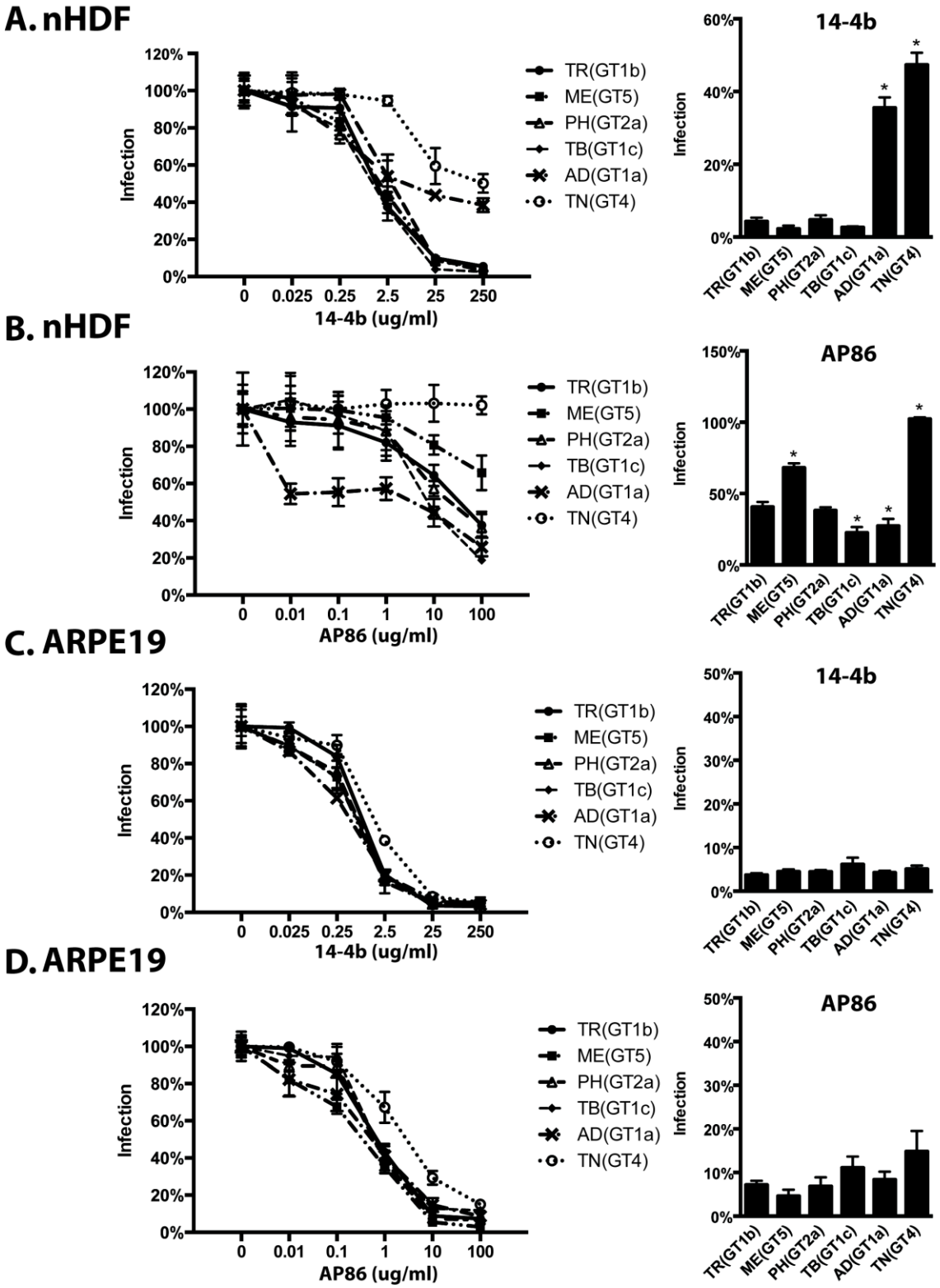

Figure 8. Neutralization of parental HCMV TR and heterologous gO recombinant by anti-gH antibodies. Equal numbers of extracellular HCMV TR or the corresponding heterologous gO recombinants were incubated with 0.025-250 μg/mL of anti-gH mAb 14-4b, or 0.01-100 μg/mL of anti-gH mAb AP86 and then plated on cultures of nHDF fibroblasts (A and B) or ARPE19 epithelial cells (C and D). At 2 days post infection the

number of infected (GFP+) cells was determined by flow cytometry and plotted as the percent of the no antibody control. (Left panels) Full titration curves shown are representative of three independent experiments, each performed in triplicate. (Right panels) Average percent of cells infected at the highest antibody concentrations in 3 independent experiments. Error bars represent standard deviations. P-values were generated by unpaired, two-tailed t-test comparing each heterologous gO recombinant to the corresponding parental virus (*<0.05).

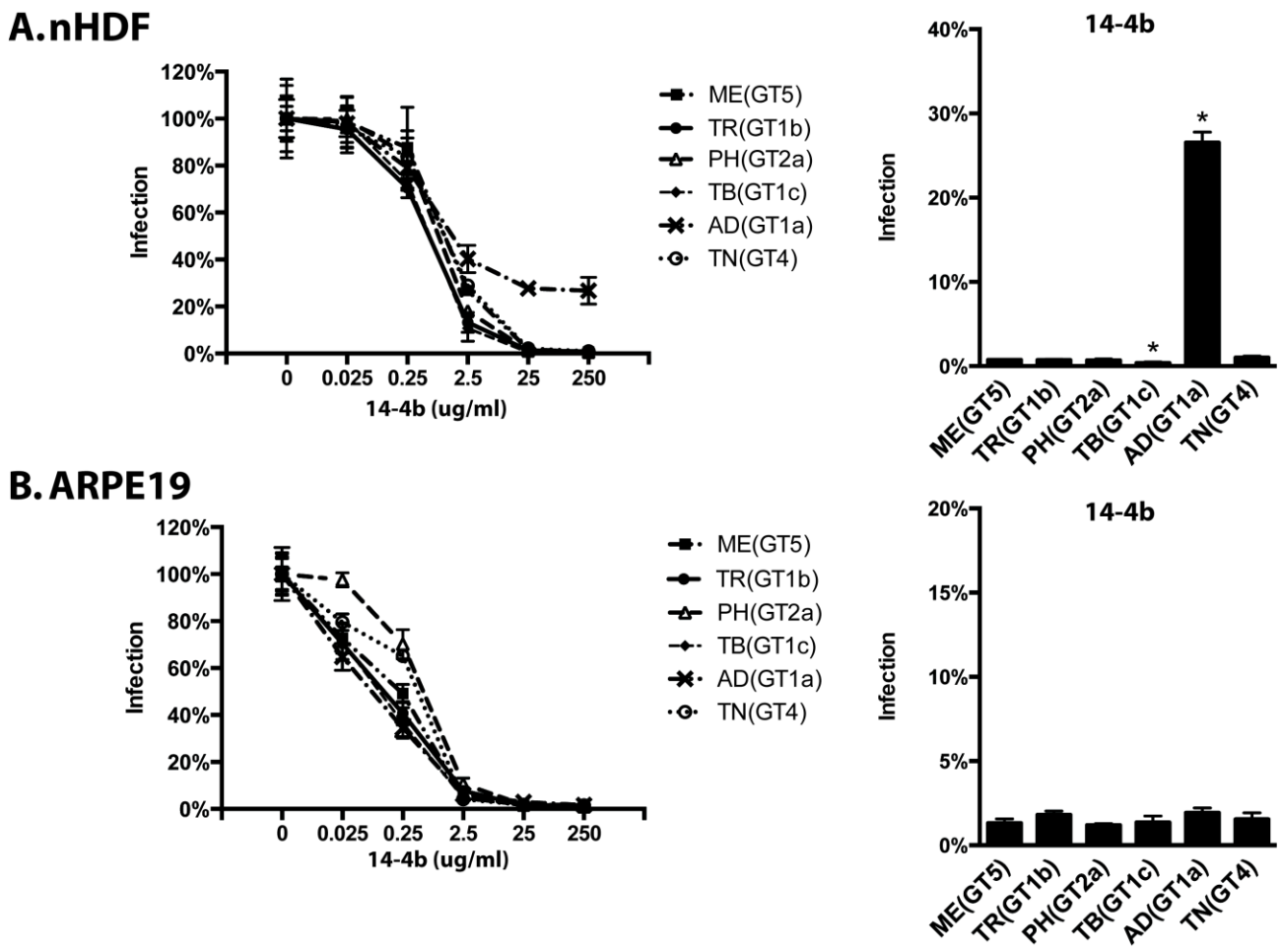

Figure 9. Neutralization of parental HCMV MT and heterologous gO recombinant by anti-gH antibodies. Equal numbers of extracellular HCMV MT or the corresponding heterologous gO recombinants were incubated with 0.025-250 μg/mL of anti-gH mAb 14-4b and then plated on cultures of nHDF fibroblasts (A) or ARPE19 epithelial cells (B). At 2 days post infection the number of infected (GFP+) cells was determined by flow cytometry and plotted as the percent of the no antibody control. (Left panels) Full titration curves shown are representative of three independent experiments, each performed in triplicate. (Right panels) Average percent of cells infected at the highest antibody concentrations in 3 independent experiments. Error bars represent standard deviations. P-values were generated by unpaired, two-tailed t-test comparing each heterologous gO recombinant to the corresponding parental virus (*<0.05).